The influence of Tissue Responses on the Electrochemical properties of Implanted Neural Stimulation Electrodes

Meijs, Suzan

DOI (link to publication from Publisher):
10.5278/vbn.phd.med.00046

Publication date:
2015

Document Version
Publisher's PDF, also known as Version of record

THE INFLUENCE OF TISSUE RESPONSES ON THE ELECTROCHEMICAL PROPERTIES OF IMPLANTED NEURAL STIMULATION ELECTRODES

BY
SUZAN MEIJS

DISSERTATION SUBMITTED 2015

AALBORG UNIVERSITY
DENMARK

THE INFLUENCE OF TISSUE RESPONSES ON THE ELECTROCHEMICAL PROPERTIES OF IMPLANTED NEURAL STIMULATION ELECTRODES

by

Suzan Meijs

AALBORG UNIVERSITY
DENMARK

Dissertation submitted

.

Thesis submitted:	December 21, 2015
PhD supervisor:	Prof. N. J. M. Rijkhoff Aalborg University
Assistant PhD supervisor:	Prof. T. Stieglitz Albert Ludwig University of Freiburg
	Dr. Morten Voss Fjorback Previously employed at Neurodan A/S
PhD committee:	Professor Johannes Struijk (chairman) Aalborg University
	Professor Stuart F. Cogan University of Texas at Dallas
	Professor Xavier Navarro Ecebes Universitat Autonoma de Barcelons (UAB)
PhD Series:	Faculty of Medicine, Aalborg University

ISSN (online): 2246-1302
ISBN (online): 978-87-7112-448-4

Published by:
Aalborg University Press
Skjernvej 4A, 2nd floor
DK – 9220 Aalborg Ø
Phone: +45 99407140
aauf@forlag.aau.dk
forlag.aau.dk

Printed in Denmark by Rosendahls, 2015

CV

PERSONAL DETAILS

Family name	Meijs
First name	Suzan
E-mail address	suzan.meijs@gmail.com
Telephone	+45 5252 8792

SKILLS

Through my Bachelor's education I have gained a strong **theoretical knowledge in bioelectricity and biochemistry**. My Master's education has provided me with the capacity to **set up a scientific study**, has **refined my knowledge** especially in the field of **neural prostheses** and has equipped me with practical skills to **carry out experiments** on humans.

Through my work experience, I have gained experience with **medical device safety and security**. I have learned to **write protocols** for various kinds of studies, including **human and animal experiments** and to accurately document the results of these studies in a company as well an academic setting.

The words that would describe my professional nature best are **dedication and diligence**. I do not mind to work hard to reach my objectives and I always strive to be good at what I am doing.

EDUCATION

2008 – 2010	Masters in Biomedical Engineering at the University of Aalborg, specialization in biomedical signals and systems.
2004 – 2007	Bachelors in Biomedical Engineering at the Twente University, specialization in electrical and chemical engineering.

WORK EXPERIENCE

2015 – Now	Founder of Meijs Biomed. Pre-clinical research and documentation to gain permission for clinical investigations.
2012 – Now	PhD at the center for sensory-motor interaction (SMI) at Aalborg University. Research project on electrochemical characterization of neural stimulation electrodes *in vitro* and *in vivo*. Setting up and carrying out this project independently, writing research articles and being able to place the research project and its findings in the context of the state of the art.
2010 – 2011	R&D engineer at Neurodan A/S, member of the Otto Bock group. Contributing to all parts of research and development of

	an implantable medical device, including protocol writing, animal experimentation and documentation.
2010	Research assistant at the department of health, science and technology at Aalborg University. Assisting in experimental research in motor control and brain computer interfaces.
2008 – 2009	Research assistant at the department of health, science and technology at Aalborg University. Assisting in experimental research and signal analysis for urinary bladder control.
Fall 2007	Full-time position at the department of clinical physics at the hospital 'Medisch Spectrum Twente', working on the effect of mobile phones on critical care equipment and determining the requirements for examining x-ray images.
Spring 2007	Research assistant at the department of Biomedical Signals and Systems at Twente University, designing and teaching a biomedical engineering class 'Measurements on pain'.

PUBLICATIONS

1. Meijs, S., Fjorback, M., Jensen, C., Sørensen, S., Rechendorff, K., & Rijkhoff, N. (2015). Electrochemical properties of titanium nitride nerve stimulation electrodes: an *in vitro* and *in vivo* study. *Frontiers in Neuroscience*, *9*, [268]. 10.3389/fnins.2015.00268
2. Meijs, S., Sørensen, S., Rechendorff, K., Rijkhoff, N.J.M. (2015) In Vivo Charge Injection Limits Increased After 'Unsafe' Stimulation. In *Proceedings of the 3rd neurotechnix conference*, 16-17 November 2015, Lisbon.
3. Meijs, S., McDonald, M., Sørensen, S., Rechendorff, K., Petrák, V., Nesládek, M., Rijkhoff, N.J.M., Pennisi, C.P. (2015) Increased charge storage capacity of titanium nitride electrodes by deposition of boron-doped nanocrystalline diamond films. In *Proceedings of the 3rd neurotechnix conference*, 16-17 November 2015, Lisbon.
4. Meijs, S., Sørensen, C., Sørensen, S., Rechendorff, K., Fjorback, M., & Rijkhoff, N. (2015). Comparison of the electrochemical properties of smooth and porous TiN electrode coatings in rats. In *7th IEEE EMBS Conference on Neural Engineering, 22-24 April 2015, Montpellier, France.* (pp. 486-489). IEEE Press. 10.1109/NER.2015.7146665
5. Pennisi, C. P., Alcaide, M., Papaioannou, S., Meijs, S., Taylor, A., Nesladek, M., & Zachar, V. (2014). Biocompatibility and electrochemical assessment of boron doped nanocrystalline diamond electrodes for neural stimulation. *Frontiers in Neuroengineering.* 10.3389/conf.fneng.2014.11.00005
6. Meijs, S., Fjorback, M., Sørensen, S., Rechendorff, K., & Rijkhoff, N. (2014). Increasing voltage transients using implanted titanium nitride neural stimulation electrodes. In W. Jensen, O. K. Andersen, & M. Akay (Eds.), *Replace, Repair, Restore, Relieve : Bridging Clinical and Engineering Solutions in Neurorehabilitation: Proceedings of the 2nd International Conference on NeuroRehabilitation, ICNR2014, 24-26 June 2014, Aalborg, Denmark.* (pp. 543-551). Springer. (Biosystems and Biorobotics; No. 7). 10.1007/978-3-319-08072-7_80

7. Meijs, S., Fjorback, M., & Rijkhoff, N. (2013). Chronic electrochemical investigation of titanium nitride stimulation electrodes in vivo. In J. L. Pons, D. Torricelli, & M. Pajaro (Eds.), *Converging Clinical and Engineering Research on Neurorehabilitation: International Conference on NeuroRehabilitation, ICNR 2012, 14-16 November 2012, Toledo, Spain.* (Vol. Part I, pp. 421-425). Springer Publishing Company. (Biosystems and Biorobotics, Vol. 1). 10.1007/978-3-642-34546-3_68
8. Meijs, S., Taylor, A., Pennisi, C. P., & Rijkhoff, N. (2013). *Electrochemical characterization of boron-doped nanocrystalline diamond electrodes for neural stimulation*. Abstract from International IEEE EMBS Conference on Neural Engineering, San Diego, CA, United States.
9. Meijs, S., Fjorback, M., Sørensen, S., Rechendorff, K., & Rijkhoff, N. (2013). Electrochemical investigation of peripheral nerve stimulation electrodes in vivo and in vitro during 53 days. In *Proceedings of the 6th International IEEE EMBS Conference on Neural Engineering, 6-8 November 2013, San Diego, CA, USA.* (pp. 251-254). IEEE.
10. Andersen, I. H., Sørensen, S., Rechendorff, K., Nielsen, L. P., Meijs, S., & Fjorback, M. (2012). Porous TiN coatings for improved electrode performance. In *Nano Update 2012: Programme & Abstracts.* (pp. 26). Nano Connect Scandinavia.
11. Meijs, S., Fjorback, M., Sørensen, S., Rechendorff, K., & Rijkhoff, N. (2012). *Investigation of electrochemical behavior of porous TiN stimulation electrodes in vivo*. Abstract from International Conference on Neuroprosthetic Devices, ICNPD 2012, Freiburg, Germany.
12. Sørensen, S., Andersen, I. H., Rechendorff, K., Nielsen, L. P., Meijs, S., & Fjorback, M. (2012). *Sputter deposited TiN thin film coatings for optimized electrochemical performance of neurostimulation electrodes*. Abstract from International Conference on Neuroprosthetic Devices, ICNPD 2012, Freiburg, Germany.
13. Meijs, S. Fjorback M. and Rijkhoff N.J.M (2011) In vivo impedance characterization of a monopolar extra-neural electrode. 15th Nordic-Baltic Conference on Biomedical Engineering and Medical Physics, Aalborg, Denmark.
14. Rijkhoff, N.J.M. and de Goede, S. (2009) A new method to assess the penilo-/clitoro-anal reflex. 39th Annual Meeting of the Continence Society, San Francisco, USA.

AWARDS

IFMBE Young Investigator Award, Nordic Baltic conference, 14-18 June 2011.
Best student paper award, Neurotechnix 2015, 16-17 November 2015.

LANGUAGES

Dutch	Native tongue
English	Full professional proficiency
Danish	Professional proficiency

ENGLISH SUMMARY

Electrical stimulation using implanted electrodes is used to relieve the symptoms of various diseases, among others voiding dysfunctions. After the electrodes are implanted, their electrochemical properties are markedly different compared to electrodes placed in inorganic saline.

The aim of this PhD project was to investigate the relationship between the biological responses to implantation of stimulation electrodes and the changes in the electrochemical properties of these electrodes. This was done using a conventional electrode material (titanium nitride) with different surface structures and using a novel biofouling resistant electrode material (boron-doped diamond).

Study I and II showed that the electrochemical properties of electrodes implanted and those placed in saline are different. It was also observed that the electrochemical properties of implanted electrodes change with time. Specifically, the changes of the voltages observed during electrical stimulation closely resembled the changes in tissue impedance. In study III, smooth electrodes were shown to be less affected by acute as well as chronic implantation. The difference between smooth and porous electrodes was, however, largest upon acute implantation compared to placement in saline. This means that *in vivo* electrochemical properties of porous stimulation electrodes could be improved, if the effect of protein adsorption could be decreased. Therefore, the electrochemical properties of boron-doped diamond were investigated *in vitro* and *in vivo* (study IV). Boron-doped diamond has been reported to be unaffected by protein adsorption in organic solutions. The double layer and pulsing capacitance of boron-doped diamond was unaffected by acute and chronic implantation. However, its capacitance remained lower than that of smooth titanium nitride. It was therefore investigated whether a thin layer of boron-doped diamond could be deposited on porous titanium nitride (study V). This increased its surface area more than 100-fold and thereby the capacitance.

These results hold great promise for the future as there are currently no other electrode materials with electrochemical properties that are unaffected by implantation. Future studies should investigate how porous boron-doped diamond is affected by implantation, as the surface structure influences the foreign body response. It would furthermore be interesting to investigate the application of boron-doped diamond for direct neural interfaces by tailoring it with specific proteins.

DANSK RESUME

Elektrisk stimulation med implanterede elektroder anvendes til at reducere symptomerne ved forskellige sygdomme, heriblandt vandladningsforstyrrelser. Efter implantation af elektroderne, er de elektrokemiske egenskaber meget anderledes sammenlignet med elektroder i en uorganisk saltvandopløsning.

Formålet med dette Ph.D.-projekt var at undersøge sammenhængen mellem de biologiske ændringer, der forårsages af implantationen, og ændringer i elektrodernes elektrokemiske egenskaber. Dette blev udført ved brug af et konventionelt elektrodemateriale (titaniumnitrid, TiN) med forskellige overflade-strukturer og et nyt "biofouling"-resistent elektrodemateriale (bor-beriget diamant).

Studie I og II viste, at elektrodernes elektrokemiske egenskaber var anderledes efter implantation sammenlignet med deres egenskaber i saltvand. De viste desuden en tydelig sammenhæng mellem spændingsændringer under elektrisk stimulation og ændringer i vævsimpedansen. I studie III viste det sig, at glatte elektroder var mindre påvirket af akut samt kronisk implantation. Forskellen mellem glatte og porøse elektroder var dog størst ved akut implantation sammenlignet med elektroder i saltvand. Dette betyder, at elektrokemiske egenskaber af porøse stimulationselektroder kan forbedres, hvis effekten af protein-vedhæftning mindskes. De elektrokemiske egenskaber af bor-berigede diamant elektroder blev derfor undersøgt *in vitro* og *in vivo* (studie IV). Studier af bor-beriget diamant viser, at dette ikke påvirkes af protein-vedhæftning i organiske opløsninger. Dobbeltlag- og pulskapacitans af bor-berigede diamant elektroderne blev ikke påvirket af akut eller kronisk implantation. Kapacitansen var dog lavere end for glat titaniumnitrid. Det blev derfor undersøgt, om det var muligt at deponere et tyndt lag bor-beriget diamant oven på porøs titaniumnitrid. Dette øgede overfladearealet mere end 100 gange og dermed også kapacitancen.

Disse resultater er meget lovende, da der på nuværende tidspunkt ikke er andre elektrodematerialer hvor de elektrokemiske egenskaber ikke ændres efter implantation. Fremtidige studier skal undersøge om porøs bor-beriget diamant påvirkes af implantation, da overfladestrukturen påvirker fremmedlegeme-reaktionen. Det vil yderlige være interessant at undersøge, om porøs bor-beriget diamant kan anvendes ved direkte kontakt til nerveceller gennem modifikation af overfladen med vedhæftning af specifikke proteiner.

ACKNOWLEDGEMENTS

First and foremost, I will thank my God. It is only by His grace that I have been able to carry out this work. It is through His guidance that I could keep my eyes fixed on what really is important.

Nico, I could not think of a better supervisor. The balance between freedom to design and carry out the PhD project and support in challenging situations suited me perfectly.

Morten, it has been a joy to work with you and I appreciate your honesty and openness. It has been strange to finish off the work without you.

Thomas Stieglitz, thanks for the few meetings we've had. They were very useful and typically gave me new insights.

All my co-authors, without you I could not have completed the work. Morten, Carina, Maria, Charlotte and Alana worked with me in the lab and made it a joy to do the "dirty work". Although it has been hard sometimes to get on the same wavelength, Søren and Kristian never gave up and kept working to reach our goals.

The staff at the animal facility at Aalborg University hospital, you were always willing to lend a hand and always in for an interesting conversation. Thanks for never ceasing to be as flexible as possible and thanks for all the rundstykker!

Søren Nielsen, from Aalborg University hospital's pathology department. Thank you for preparing the histological samples and for generously taking the time to explain what cells we were looking at.

Carsten Dahl Mørch, thanks for your support in all the statistical analysis.

Thanks to my family, who have always supported and encouraged me to set high goals and work as hard as possible to reach them. Especially thanks to my mother, who has shown me in so many ways what it means to love sacrificially.

Thanks to my husband. I could say a million words and more about what you have done for me in these years. But I am still most of all thankful for who you are.

Thanks to Koinonia international Christian fellowship for supporting me in every situation in love and prayer.

TABLE OF CONTENTS

TABLE OF FIGURES

CHAPTER 1. INTRODUCTION

Neural stimulation with implantable electrodes is used for many applications and stimulation can take place in the brain (Jackson & Zimmermann, 2012; Miocinovic et al., 2013; Stieglitz & Meyer, 2006; Zhou & Greenbaum, 2009), the spinal cord (Jackson & Zimmermann, 2012; Zhou & Greenbaum, 2009) as well as in the peripheral nervous system (Stieglitz & Meyer, 2006; Navarro et al., 2005; Zhou & Greenbaum, 2009). The requirements for neural stimulation electrodes depend on the intended clinical effect, the tissue in which it is implanted, the target neurons, the distance between the electrode and the target neurons, the degree of invasiveness and the feasibility to produce the electrode in a cost-effective manner (Tyler & Polasek, 2009). It is therefore important to determine the target tissue, the optimal electrode location and the implantation procedure early in the development process (Tyler & Polasek, 2009).

In this PhD project, the stimulation contact was of particular interest. The stimulation contact requires a specific design depending on the aforementioned aspects. The next section presents the system that the electrode contact is a part of, its intended clinical effect, the implantation procedure and the requirements these place on the electrode contact. Thereafter, the electrochemical properties of the most novel stimulation materials are reviewed. The aim of this PhD project was to investigate the electrochemical properties of the stimulation contact after implantation. The focus was on examining how biological responses influence the stimulation properties of the electrode. For this purpose, the literature regarding biological responses to implanted materials and how these affect *in vivo* electrochemical properties is reviewed. At the end of this chapter, an overview of the thesis is presented.

1.1. C-LIFE SYSTEM

The system, of which the electrode contact is a part, inhibits the bladder muscle reflexively on demand to prevent incontinence in patients with urge urinary incontinence. For this purpose the stimulation electrode is placed at the distal end of the dorsal genital nerve (Farag et al., 2012; Fjorback et al., 2006; Van Breda et al., 2014). This has the advantage of specificity, as only afferents from the genitals are stimulated to obtain reflexive inhibition of the bladder. It further has the advantage of accessibility, as the genital nerves are fairly superficial in men and women and can be stimulated using skin, needle and implanted electrodes (Farag et al., 2012; Martens, 2011; Van Breda et al., 2014). Due to this, an electrode can be implanted close to the nerve using a minimally invasive stimulation guided technique (see Figure 1-1) (Martens et al., 2011, Van Breda et al., 2014). The entire system, as it's intended to be developed is shown in Figure 1-2.

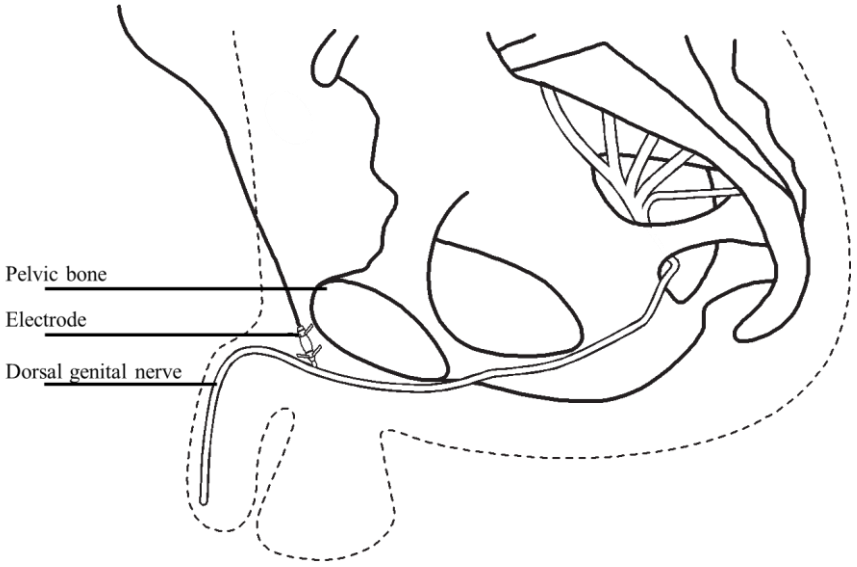

Figure 1-1 Electrode as it would be implanted in a male (used with permission from Neurodan A/S).

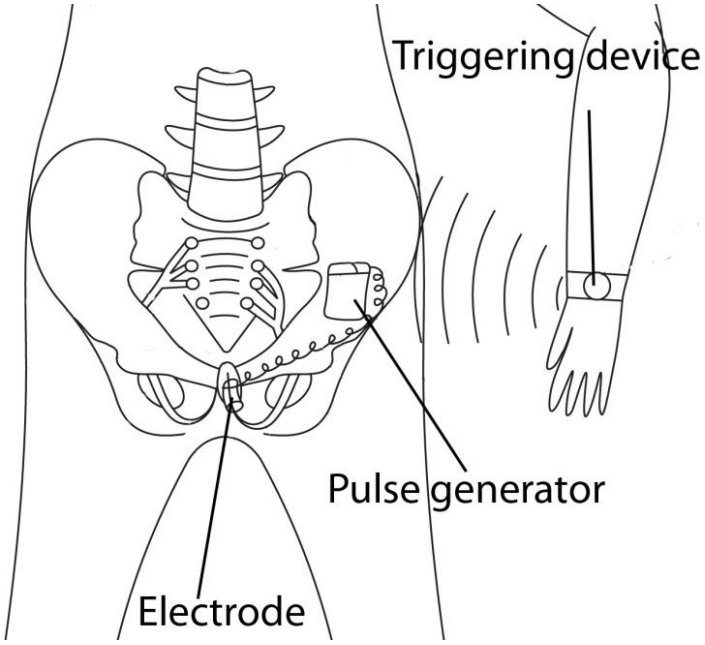

Figure 1-2 The entire system consists of an electrode, an implantable pulse generator and a device by which the user can trigger stimulation (from Fjorback et al. (2009), with permission).

The location and implantation of the electrodes, as well as its intended clinical effect places certain demands on the electrode contact (Tyler & Polasek, 2009). To obtain the desired clinical effect -immediate suppression of a bladder contraction- the maximum stimulation current that patients can tolerate is used. This demands that it should be possible to inject a minimum charge of 5 μC safely and reversibly (Goldman et al., 2008; Martens et al., 2011)[1]. At the same time, the electrode should be as small as possible to cause as little damage as possible during minimally invasive implantation. However, the amount of charge that can be delivered safely and reversibly is smaller when the surface area is smaller. It is therefore advantageous to increase the surface area of the electrode contact, without increasing the dimensions of the electrode.

The electrode contact as well as the electrode in general should be designed for manufacturability, biocompatibility, (mechanical and chemical) stability and safety. Since the expected lifetime of the electrode may exceed 10 years, the material must be resistant to (stimulation induced) corrosion.

A titanium, aluminum, vanadium (Ti6Al4V) alloy was selected as a substrate material, because it is a commonly used material in medical implants. It is therefore known to be biocompatible and mechanically stable. However, this substrate is not capable of injecting the required amount of charge and therefore a surface treatment should be applied. The geometry of the electrode contact had also been determined before the start of the PhD study (see Figure 1-3). The stimulation contact has a length of 1.6 mm to make it robust against small movements.

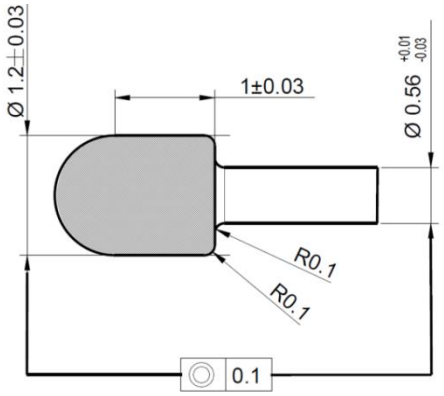

Figure 1-3 The dimension of the stimulating contact of the electrode (shaded area); measures are in mm (used with permission from Neurodan A/S).

[1] Goldman et al. (2008) and Martens et al. (2011) mention 24 mA and 25 mA as the highest maximum tolerable current, respectively. A charge of 5 μC is obtained by multiplying a current of 25 mA with a pulse width of 200 μs, in accordance with Martens et al. (2011).

1.2. STATE-OF-ART IN ELECTRODE MATERIALS

As mentioned in the previous section, a surface treatment should be applied to the Ti6Al4V substrate to increase the amount of charge that can be injected safely and reversibly. The charge injection capacities (Q_{inj}) listed in Table 1-1 suggest, however, that almost any of the materials could inject the required amount of charge (0.083 mC/cm^2). Most of the electrodes mentioned in Table 1-1 are micro-electrodes. Since Q_{inj} decreases with increasing geometrical surface area (GSA), Q_{inj} cannot be applied directly to macro-electrodes (Cogan et al., 2009). Two macro-electrodes are encircled in red in Table 1-1. One has indeed a relatively small Q_{inj} (0.034-0.054 mC/cm^2) (Leung et al., 2015), while the other has a relatively large Q_{inj} (> 0.7 mC/cm^2) (Terasawa et al., 2013). The large Q_{inj} is due to roughening of the electrode surface, increasing its electrochemical surface area (ESA) while maintaining the same GSA (Terasawa et al., 2013).

The surface structure of a material can be adjusted in various ways in order to increase the ESA/GSA ratio. Increasing the ESA typically results in increased stimulation and sensing performance. The electrode substrate material can be roughened using mechanical or chemical methods. Alternatively, additional organic (conducting polymers, carbon nanotubes, conductive hydrogels, diamond) or inorganic (platinum (Pt), iridium oxide (IrOx), titanium nitride (TiN)) coatings can be applied to the substrate (Aregueta-Robles, 2014; Heim et al., 2012). Recently, the effect of combining two different coatings has been investigated. Examples of this are: carbon nanotubes (CNT) and IrOx (Carretero et al., 2014), CNT and poly-3,4-ethylenedioxythiophene (PEDOT) (Luo et al., 2011; Samba et al., 2015; Zhou et al., 2013), PEDOT and graphene oxide (GO) (Tian, 2014a), PEDOT and hydrogels (Cheong et al., 2014), IrOx and GO (Carretero et al., 2015), CNT and diamond (Hebert et al., 2014) and diamond and metal coatings (Garret et al., 2012).

The goal of most of these efforts is to increase Q_{inj} by increasing the ESA of the electrode. Increased Q_{inj} allows for miniaturization of the electrode contact. This is especially desirable for applications like visual and auditory prostheses, as it may facilitate a higher resolution of vision and sound (Zhou & Greenberg, 2011). For dorsal genital nerve stimulation, increased Q_{inj} makes it possible to excite the nerve at greater electrode-nerve distances. This may make the minimally invasive implantation more likely to succeed, as the electrode-nerve distance is less critical.

By adjusting the surface structure to increase Q_{inj}, the ESA/GSA ratio is increased (Zhou & Greenberg, 2011). However, not the entire ESA can be used under fast pulsing conditions due to a time constant for accessing the entire pore depth (Cogan, 2008). This time constant is influenced by the electrode material, the electrolyte and the pore size (Cogan, 2008). This thesis focuses on the electrolyte, and more specifically how changes in the tissue influence the electrochemical properties (such as Q_{inj}) of implanted electrodes.

Table 1-1 Charge injection capacity (Q_{inj}) of various electrode materials at their equilibrium potential in saline. Besides the variations in potential limits and pulse width, the electrolyte, temperature and surface area may vary between and within the studies mentioned.

Material	Cathodal limit	Q_{inj} (mC/cm^2)	Pulse width	Source
TiN	-0.6 V vs. Ag|AgCl	0.87	100 µs	Weiland et al., 2002
	-1.2 V vs. Ag|AgCl	2.2-3.5	1 ms	Zhou & Greenberg, 2003
	-1.0 V	0.2	300 µs	Aryan et al., 2011
	-0.8 V vs. Ag|AgCl	0.43	500 µs	Pan et al., 2013
Pt	-0.6 V vs. Ag|AgCl	0.3	200 µs	Negi et al., 2010
Porous	-0.6 V vs. Ag|AgCl	3	400 µs	Park et al., 2010
PtIr	-0.6 V vs. Ag|AgCl	0.13	1 ms	Venkatraman et al., 2011
Porous	-0.6 V vs. Ag|AgCl	> 0.7	500 µs	Terasawa et al., 2013
	-0.6 V vs. Ag|AgCl	0.034 0.054	100 µs 3.2 ms	Leung et al., 2015
Porous	-0.6 V vs Ag|AgCl	0.5	200 µs	Kim & Nam, 2015
Porous	-0.6 V vs Ag|AgCl	0.55 1.0	200 µs 400 µs	Weremfo et al., 2015
IrOx	-0.6 V vs. Ag|AgCl	4	100 µs	Weiland et al., 2002
Activated	-0.6 V vs. Ag|AgCl	0.9	400 µs	Cogan et al., 2006
	-0.6 V vs. Ag|AgCl	1.9-4.4	400 µs	Cogan et al., 2009
	-0.6 V vs. Ag|AgCl	2.0	200 µs	Negi et al. 2010a
	-0.6 V vs. Ag|AgCl	0.19	1 ms	Venkatraman et al., 2011
	-0.6 V vs. Ag|AgCl	0.7	500 µs	Pan et al., 2013
Diamond	-1.1 V vs. Ag|AgCl	0.02-0.16	1 ms	Garret et al., 2012
	-0.47 V vs. Ag|AgCl * Pulse clamp method	0.003	100 µs	Kim, 2014
CNT	-0.9 V vs. Ag|AgCl	0.1-0.7	1 ms	Brown et al., 2011
PEDOT-CNT	-0.7 V vs. Ag|AgCl	2.5	1 ms	Luo et al, 2011
	-0.6 V vs. SCE	5.6-6.2	200 µs	Zhou et al., 2013
PEDOT	-0.6 V vs. Ag|AgCl	2.92	1 ms	Venkatraman et al., 2011
	-0.6 V vs Ag|AgCl	1.2 3.9	100 µs 800 µs	Green et al., 2013a
	-0.6 V vs. Ag|AgCl *Different PEDOT dopants	0.7-5.6	1 ms	Tian et al., 2014b
	-0.6 V vs Ag|AgCl	1.4	200 µs	Guex et al., 2015
Polypyrrole	-0.6 V vs. SCE	3.2-7.5	200 µs	Lu et al., 2010
Hydrogel	-0.6 V vs Ag|AgCl	0.81-0.83	200 µs	Green et al., 2013b
	-0.6 V vs Ag|AgCl	0.085 2.41	25 µs 800 µs	Hassarati et al., 2014

1.3. BIOLOGICAL RESPONSES TO IMPLANTS

The electrochemical properties of implanted electrodes are dramatically different than the properties of these electrodes in inorganic saline. The adhesion of proteins and cells to the electrode surface changes the way charge is injected (Lempka et al., 2009; Newbold, 2010). In this section, the tissue responses to electrode implantation and the effect of these on the electrochemical properties of the implanted electrode are reviewed.

Upon acute implantation, proteins and some cells adsorb to the electrode surface and a provisional matrix is formed around the implant. This is the first step towards wound healing and foreign body reaction (Anderson et al., 2008). Protein adsorption alone leads to minimal changes in the impedance spectrum (Lempka et al., 2009). However, comparing the impedance spectrum of implanted electrodes to the impedance spectrum of electrodes in saline, several differences are observed. The high-frequency (electrolyte) impedance is increased, primarily due to the bulk tissue resistance (Cogan, 2006; Mandal et al., 2015; Minikanti et al., 2010; Wei & Grill, 2009). Additionally, a decrease in the low-frequency (electrode) impedance has also been observed (Cogan, 2006; Wei & Grill, 2009). The appearance of the cyclic voltammogram (CV) is also different *in vivo* compared to *in vitro* for electrodes that inject charge via faradic pathways (Cogan, 2006; Leung et al., 2015; Minikanti et al., 2010; Musa et al., 2009). This is due to a different buffering capacity of the tissue compared to the buffering capacity of inorganic saline (Cogan, 2006; Cogan et al., 2007a). The most important differences between *in vivo* and *in vitro* measurements for stimulation electrodes are the greater electrode polarization during stimulation and the smaller Q_{inj} *in vivo* compared to *in vitro* (Brunton et al., 2015; Cogan, 2006; Green et al., 2013; Leung et al., 2015 Wei & Grill, 2009). Increased electrode polarization during electrical stimulation has also been observed *in vitro* in albumin solution (Newbold et al., 2010).

After provisional matrix formation, a stage of acute inflammation follows, characterized by the presence of neutrophils (Anderson et al., 2008). Neutrophils are the most abundant type of white blood cells and are part of the innate immune system. Another characteristic aspect of the acute inflammation phase is the degranulation of mast cells, releasing their histamines and fibrinogens, which influences the extent of the foreign body response (Anderson et al., 2008). The acute inflammation phase last approximately one week and is associated with low tissue impedances (Grill & Mortimer, 1994; Williams et al., 2007).

The presence of mononuclear leukocytes, such as macrophages and lymphocytes, is indicative of the chronic inflammation stage (Anderson et al., 2008). The corresponding increase in cell density near the electrode contact causes an increase in the high-frequency tissue impedance (Lempka et al., 2009; Williams et al.,

2007). The duration of acute and chronic inflammation for biocompatible materials is typically 2 weeks (Anderson et al., 2008). In the presence of a foreign material, the macrophages recruit fibroblast and endothelial cells; marking the beginning of the healing and encapsulation phase (Anderson & McNally, 2011). Depending on the implanted material and its topography, a dense or a loose fibrous capsule may be formed (Anderson & McNally, 2011; Grill & Mortimer, 1994). The dense fibrous capsule leading to higher impedance values than the loose capsule composed of various cell types (Grill & Mortimer, 1994).

The cyclic voltammogram shows more resistive properties several weeks after implantation (Cogan, 2008; Kane et al., 2011). This is due to adsorption of biomolecules and fibrous encapsulation of the electrode (Cogan, 2008), but at which stage the cyclic voltammogram becomes more resistive and how this is related to the foreign body response is unknown. Increasing electrode potentials during stimulation have also been observed after implantation (Kane et al., 2011; Kane et al., 2013; Leung et al., 2015; Mandal et al., 2015; Terasawa et al., 2013; Venkatraman et al., 2011). But it is currently unknown whether this is related to tissue responses.

1.4. AIM OF THE PHD PROJECT

The previous section shows that the biological response to implantation of an electrode and the changes it causes in the impedance spectrum with time is well documented. This can be used to follow the biological response to the electrodes while they are implanted. What is not well established is the influence of changes in the tissue on the stimulation properties of implanted electrodes.

The overall aim of this PhD project was to investigate how the electrochemical properties of implanted stimulation electrodes change as a function of time after implantation. We then aimed to relate these changes to the foreign body response using electrochemical impedance spectroscopy. We suspected that porous electrodes could be more susceptible to changes in the biological environment than smooth electrodes. We investigated this with the aim to learn at which stage porous electrodes were more affected and so to optimize the porous coatings. We furthermore explored a material of which the capacitance was unaltered in protein containing solutions (biofouling resistant).

1.5. THESIS AT A GLANCE

	Research question	**Conclusion**
Study I	Does Q_{inj} of porous TiN electrodes change after implantation?	Yes, but we suspect that these subside after several weeks.
Study II	Can changes in Q_{inj} after implantation be related to the foreign body reaction?	Yes, electrode potentials increased up to 3-4 weeks after implantation and then stabilized.
Study III	Are smooth and porous TiN electrodes differently affected by implantation? Are smooth and porous TiN electrodes differently affected by the foreign body reaction?	Yes, electrode potentials of porous electrodes decreased a factor 3 more than electrode potentials of smooth electrodes directly after implantation. Yes, the porous electrodes show a greater decrease in electrode potentials in the chronic phase than the smooth electrodes, but the trend as a function of time is similar.
Study IV	Does a fouling resistant material (diamond) respond differently to acute implantation than TiN? Does a fouling resistant material (diamond) respond differently to the foreign body reaction than TiN?	Yes, *in vivo* electrode potentials are not larger than *in vitro* electrode potentials for diamond. Yes, electrode potentials of implanted diamond remain stable as a function of time.
Study V	Can the large ESA of porous TiN be utilized to increase the capacitance of diamond?	Yes, the capacitance of the resulting porous diamond is in the range of the capacitance of porous TiN.

CHAPTER 2. INTRODUCTION OF ELECTROCHEMICAL METHODS

In order to discuss the results of the studies, it is important to establish a level of understanding of the applied methods first. All the electrochemical methods that are described are applied in a 3-electrode cell in saline. The setup consists of the electrode under investigation termed the working electrode, a non-current carrying electrode with a known potential called the reference electrode and a large surface area counter electrode to close the electric circuit. A two-electrode set-up is used when the electrodes are implanted, consisting of the working electrode and a large surface area counter electrode of the same material.

2.1. ELECTROCHEMICAL IMPEDANCE SPECTROSCOPY

Electrochemical impedance spectroscopy (EIS) is used to investigate the electrical behavior of an electrode over a broad range of frequencies. A sinusoidal signal (voltage or current) is applied at the specified frequencies and the response (current or voltage, depending on the input) is measured. This is a very powerful method, as a small and non-destructive signal can be used to acquire information about the electrode, the electrolyte and the electrode-electrolyte interface.

Figure 2-1 shows at which frequencies the electrolyte impedance is dominant over the electrode impedance. The specific frequency up to which the electrode impedance is dominant and from which the electrolyte impedance is dominant depends on the electrode material, the ESA/GSA ratio and the electrolyte. At the highest frequencies, the electrolyte impedance is dominant. This is due to shunting of the double layer capacitance at the electrode-electrolyte interface (Wei & Grill, 2009). For electrodes immersed in inorganic saline, which is purely resistive, the phase angle is zero at frequencies where the electrolyte impedance is dominant. The phase angle of the tissue impedance, however, does not necessarily approach 0, as tissue has capacitive properties (Gabriel et al., 1996; Grill & Mortimer, 1994). As mentioned in the previous chapter, the tissue impedance can be used to follow the inflammatory response after implantation (Grill & Mortimer, 1994).

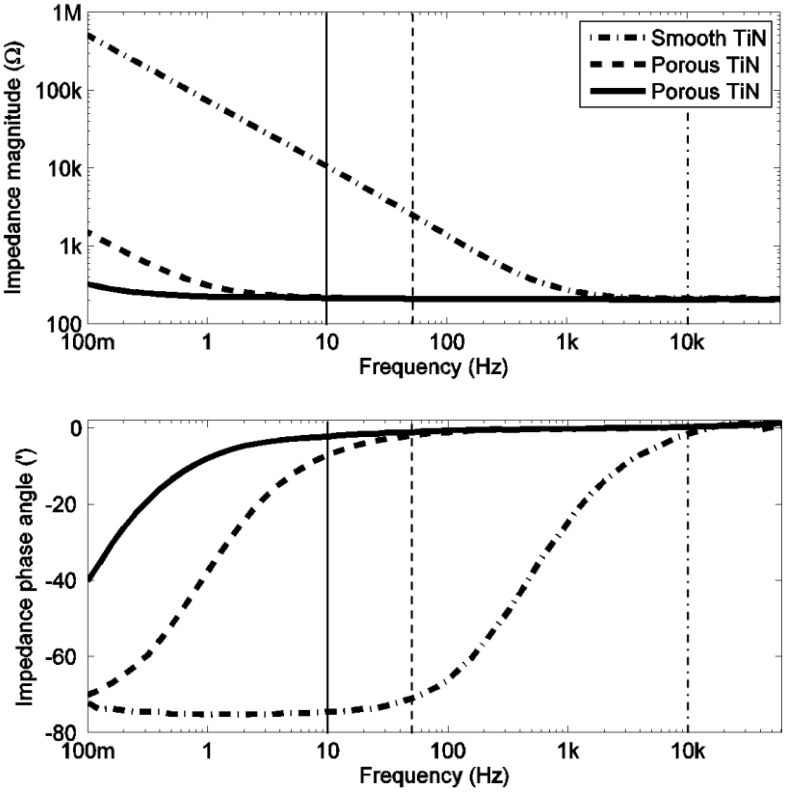

Figure 2-1 Impedance magnitude (top) and phase angle (bottom) of smooth and porous TiN electrodes measured in saline. The vertical lines indicate above which frequency the electrolyte impedance is dominant in the frequency spectrum.

The impedance spectrum can also be presented with a complex plane graph, as shown in Figure 2-2. In saline and directly after implantation, there is a linear relationship between the real and imaginary impedance. As the inflammatory response progresses, a semi-circular arc appears (Williams et al., 2007). This is due to cell adhesion to the electrode surface, introducing a capacitive component at the highest frequencies (Lempka et al., 2009; Williams et al., 2007).

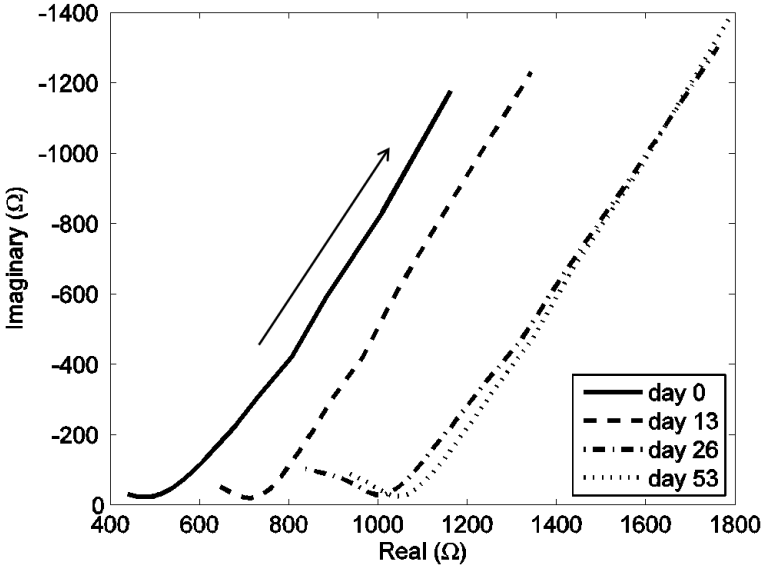

Figure 2-2 Impedance spectrum of an implanted electrode plotted in the complex plane. The arrow indicates decreasing frequency.

2.2. CYCLIC VOLTAMMETRY

Cyclic voltammetry (CV) is used to investigate how an electrode material interacts with the electrolyte. A slowly increasing and decreasing potential is applied, allowing current to flow between the working and the counter electrode. Charging of the double layer capacitance results in a stable current at varying potentials, while faradic reactions result in current peaks at distinct potentials. The potential at which such peaks occur is the reaction potential for the concerned redox reaction, while the current represents the reaction rate.

The potential limits for CV are typically the potentials at which water reduction and oxidation occur, termed the water window (Cogan, 2008). These limits are identified by an exponentially increasing current (Aryan et al., 2015). A more appropriate term would be safe potential window, as reactions that damage tissue or electrode occurring within the water window limits should also be avoided. The rate at which the potential is increased and decreased is called the sweep rate. At low sweep rates (< 100 mV/s), cyclic voltammetry is considered a near steady-state method. The double layer capacitance (C_{dl}) can be derived from the cyclic voltammogram by dividing the capacitive current (I_c) by the sweep rate ($\frac{\partial V}{\partial t}$):

$$I_c = C_{dl}\frac{\partial V}{\partial t} \quad (1)$$

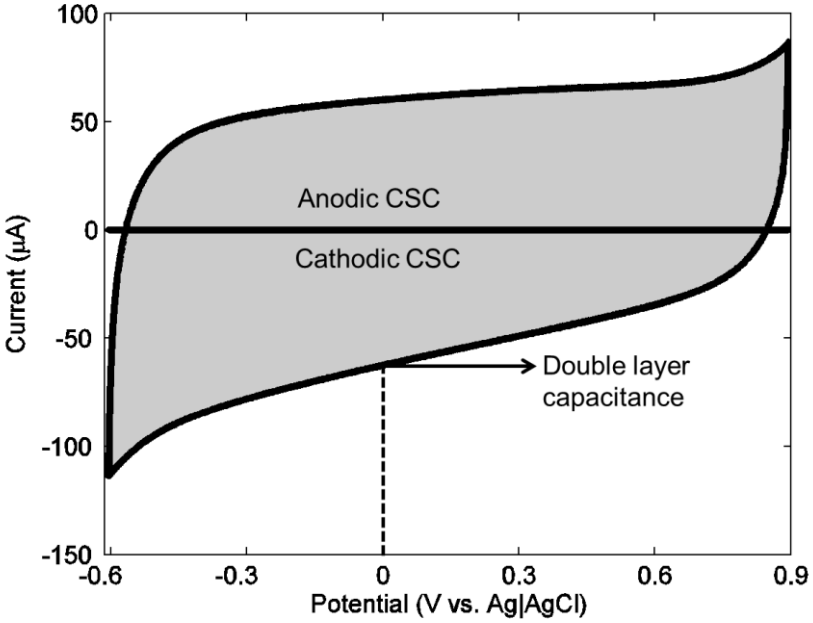

Figure 2-3 Cyclic voltammogram of a porous TiN electrode. The shaded areas above and below the 0 A axis represent the anodic and cathodic CSC, respectively. The current at 0 V is often used to calculate the double layer capacitance.

The cathodic and anodic charge storage capacity (CSC) are the surface area under or over the 0 A axis, respectively (see Figure 2-3). The CSC at slow sweep rates is representative of the ESA available for charge storage. The ESA/GSA ratio of a porous electrode can be obtained by dividing the CSC of the porous electrode by the CSC of the smooth electrode (Cogan, 2008).

With increasing sweep rates, a time constant limits the pore depth available for pulsing (Cogan, 2008; Norlin et al., 2005). This becomes apparent in the cyclic voltammogram becoming more diagonal (Norlin et al., 2005), as shown in Figure 2-4. This property is valuable when comparing electrodes of the same material with different pore depth/width. A large CSC at high sweep rates is an indication of a higher Q_{inj} during pulsing. CV, however, remains a relatively slow method (~ V/s) compared to pulsed stimulation (~kV/s).

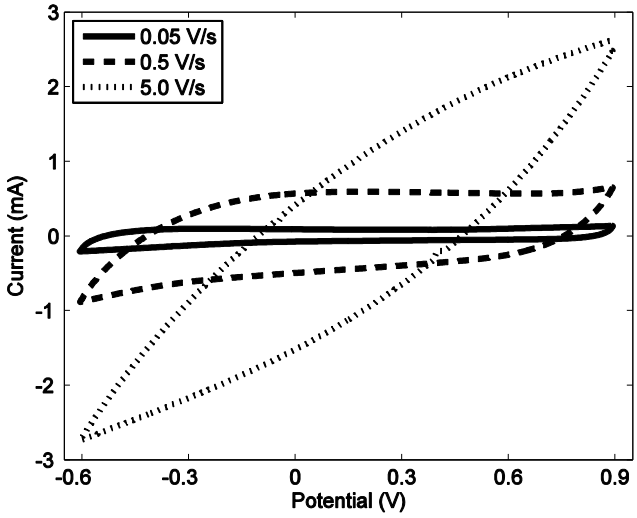

Figure 2-4 Cyclic voltammogram of a porous TiN electrode at different sweep rates. The voltammogram displays predominantly resistive properties at a sweep rate of 5.0 V/s.

2.3. VOLTAGE TRANSIENT MEASUREMENT

Voltage transient measurement (VTM) is used to investigate the electrodes' pulsing capacity. A (biphasic) stimulation current is applied and the resulting potential at the electrode interface is measured (see Figure 2-5). The instantaneous potential drop (V_a) when applying the stimulation current (I_{stim}) is due to the electrolyte or access resistance (R_a) and is called IR-drop:

$$R_a=V_a/I_{stim} \quad (2)$$

This is usually subtracted from the voltage transient, as it does not contribute to the polarization across the electrode-electrolyte interface (ΔE_p). It is ΔE_p relative to the inter-pulse potential (E_{ipp}) that make up the maximum negative and positive potential (E_{mc} and E_{ma}, respectively):

$$E_{mc} = \Delta E_p + E_{ipp} \quad (3)$$

When E_{mc} and E_{ma} exceed the safe potential limits (determined using CV), the maximum current that can be applied using the specific stimulation pulse is reached. The charge injection limit (Q_{inj}) is found by multiplying the maximum current (I_{max}) with the applied pulse width (t_p). This is typically divided by the GSA of the electrode to facilitate comparison with the literature.

$$Q_{inj} = \frac{I_{max} \cdot t_p}{GSA} \quad (4)$$

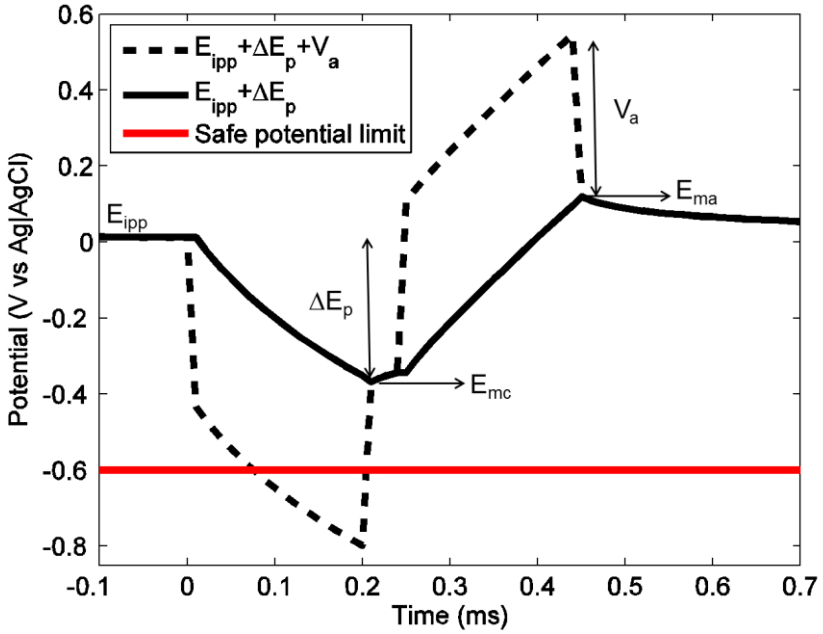

Figure 2-5 Voltage transient of a smooth TiN electrode, showing how E_{mc} depends on E_{ipp} and ΔE_p.

The pulsing capacitance (C_{pulse}) can be derived from the voltage transient using equation (1):

$$I_{stim} = C_{pulse} \frac{\partial V}{\partial t} \quad (5)$$

Where $\frac{\partial V}{\partial t}$ is the slope of the voltage transient.

With the described method, the potentials observed under fast pulsing conditions are compared to a potential limit found using a steady state method. For iridium oxide electrodes this method has given very accurate results (Cogan et al., 2004; Negi et al., 2010b). For platinum, stainless steel and gold, on the other hand, it seems to underestimate the actual charge injection limit (Bonner et al., 1993; Cogan et al., 2007b; Musa et al., 2010; Musa et al., 2011).

CHAPTER 3. INFLUENCE OF IMPLANTATION ON POROUS TITANIUM NITRIDE COATINGS

The purpose of study I and II was to investigate whether stimulation properties of titanium nitride (TiN) electrodes change after implantation. Based on results from study I, we hypothesized that the observed increase in ΔE_p (to more negative values) could be caused by changes in the tissue surrounding the electrode, namely the foreign body reaction. EIS was used to follow the tissue responses *in vivo*. An *in vitro* setup was used to follow the electrode properties in the absence of tissue responses.

Figure 3-1 shows the expected low impedance in the first week after implantation, followed by a steep increasing trend up to 3 weeks after implantation. Thereafter, a less steep increasing trend is observed, all of which is in accordance with the data reported by Grill & Mortimer (1994). The complex plane plot (see Meijs et al., *under review*; study II) shows the same increasing trend in real impedance. It also shows an increasing semi-circular arc during the first 3 weeks, which is caused by the capacitive properties of cells adhering to the electrode surface (Lempka et al., 2009; Williams et al., 2007). This also stabilized after 3 weeks of implantation.

With time, ΔE_p followed a similar trend as the impedance properties (see Figure 3-2). Smaller (less negative) ΔE_p values are observed in both studies in the first 1-2 weeks after implantation, while greater (more negative) ΔE_p values are observed after 3-4 weeks. The timespan is consistent with the durations of provisional matrix formation (minutes to days) and acute and chronic inflammation (up to 2 weeks), after which healing and encapsulation take place (Anderson et al., 2008). A dense fibrous capsule was found at the end of both studies. Its formation caused a steep increasing trend in tissue impedance and development of a semi-circular arc in the complex plane. The changes in ΔE_p occurred at the same time, making it reasonable that the changes in ΔE_p are also caused by the foreign body reaction.

The electrodes immersed in inorganic saline showed neither changes in the electrolyte impedance nor in the VTM, which confirms that reported changes are due to biological processes. In addition, ΔE_p was at the pre-implantation level when the electrodes were measured in saline again after explantation (see Table 3-1). Table 3-1 shows how remarkably similar the pulsing properties of the two different TiN coatings are. Their CSC, $C_{dl,}$ and low frequency impedance properties were incomparable. During pulsing, however, the same surface area was available for both electrode coatings *in vitro* and *in vivo*.

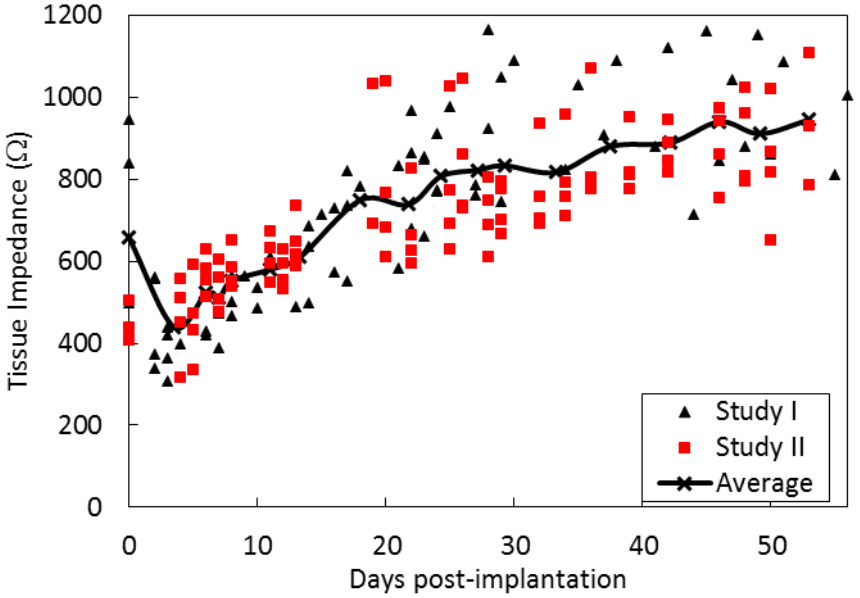

Figure 3-1 Tissue impedance (real impedance magnitude at 10 kHz) from study I and II. The average is made by averaging the data of the 2 studies. In some instances data of several days is averaged in order to always have an average with data from both studies. In those cases the x-axis data was also averaged.

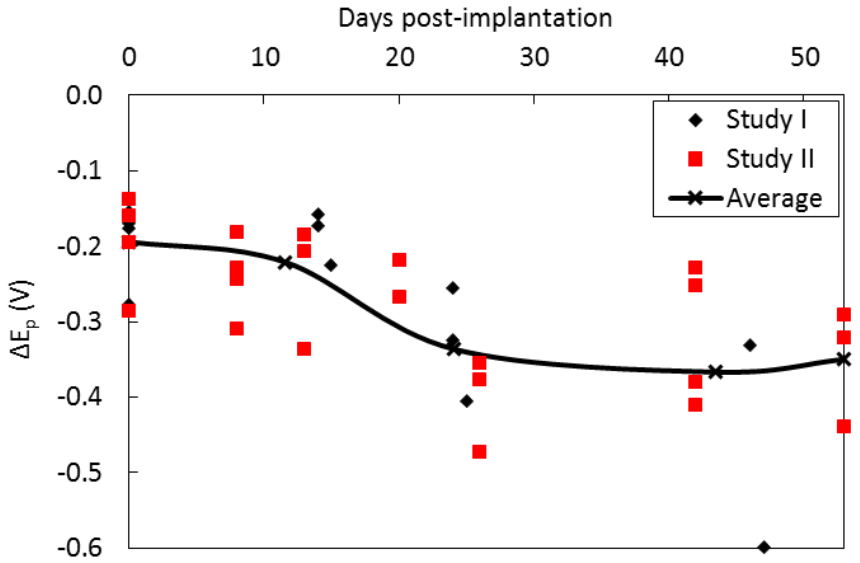

Figure 3-2 ΔE_p calculated from VTM data of study I and II. Data of several days is usually averaged in order to include data from both studies. X-axis data was also averaged.

Table 3-1 Pulsing properties in vitro (pre- and post-implantation) and in vivo (acute and chronic) of the TiN electrodes used in study I and II. The chronic data was averaged after 3 weeks of implantation to 53 days of implantation.

	Pre-implantation	**Acute**	**Chronic**	**Post-implantation**
ΔE_p (V)	0.025 ± 0.003 (n=8)	0.16 ± 0.03 (n=8)	0.36 ± 0.02 (n=16)	0.028 ± 0.002 (n=7)
- Study I	0.026 ± 0.001 (n=4)	0.19 ± 0.03 (n=4)	0.38 ± 0.06 (n=5)	0.024 ± 0.001 (n=4)
- Study II	0.023 ± 0.006 (n=4)	0.12 ± 0.04 (n=4)	0.35 ± 0.02 (n=11)	0.033 ± 0.007 (n=3)
C_{pulse}	1. 0 ± 0.1 (n=8)	0.14 ± 0.01 (n=8)	0.14 ± 0.01 (n=15)	0.8 ± 0.1 (n=7)
- Study I	0.98 ± 0.04 (n=4)	0.12 ± 0.02 (n=4)	0.11 ± 0.02 (n=5)	0.87 ± 0.05 (n=4)
- Study II	1.0 ± 0.2 (n=4)	0.15 ± 0.02 (n=4)	0.16 ± 0.01 (n=10)	0.7 ± 0.1 (n=3)

The increase in ΔE_p and C_{pulse} immediately after implantation is in line with what has been described for other implantable electrodes of various materials and in different animal models. Only the most relevant studies are mentioned in this short discussion. Brunton et al. (2015) found a smaller Q_{inj} for porous TiN electrodes after acute implantation in the rat cortex compared to the same electrodes in saline. The difference Brunton et al., found was less (factor 3) than the differences shown in Table 3-1 (Brunton et al., 2015). Clinical deep brain stimulation electrodes were investigated in cats (Wei & Grill, 2009). A significant difference in ΔE_p was observed between these electrodes in saline and implanted in the brain (Wei & Grill, 2009). Kane et al. (2013) found a smaller Q_{inj} for iridium oxide electrodes implanted in cat cortex as compared to the same electrodes placed in saline. They also described decreasing E_{mc} as a function of time after implantation, using a positive potential bias. This means that E_{ipp} remained constant and trends in ΔE_p can be compared directly to trends in E_{mc} (Kane et al., 2013). Leung et al. (2015) found great decreases in Q_{inj} after implantation compared to *in vitro* for smooth platinum electrodes. The electrodes were implanted in the rat cortex, the cochlea and the eye and differences were also found between the implantation sites (Leung et al., 2015). This indicates that the amount of change in Q_{inj} directly after implantation compared to placement in saline is dependent on the type of tissue the electrode is surrounded with.

All studies used a different setup, different electrodes, different animals and different implantations sites. However, in all animals and at all implantation sites, a

decrease in Q_{inj} or an increase in ΔE_p has been observed after acute implantation, which is also the case for other studies that are not mentioned here. This is most likely due to protein adsorption to the electrodes, which increases ΔE_p even in saline (Newbold et al., 2010). Furthermore, E_{mc} continued to increase as a function of time after implantation for iridium oxide electrodes implanted in the cat cortex (Kane et al., 2013). On the other hand, a significant difference in Q_{inj} was not found for smooth platinum electrodes that had been implanted in the suprachoroidal space in the rat for 3 months compared to directly (within 72 hours) after implantation (Leung et al., 2015). Again, these studies are vastly different in their setup, animal model, implantation site and electrode materials. Our studies are unique in attempting to relate the changes in Q_{inj} and ΔE_p to changes in the tissue. The earliest electrochemical data in the aforementioned studies is recorded on day 33 (Kane et al., 2013). No histological data is presented in either of the studies to judge how the tissue may have affected the electrochemical results (Kane et al., 2013; Leung et al., 2015), which makes it difficult to compare the results of these studies to ours.

In conclusion, the greatest changes in pulsing properties occur directly after implantation and are likely due to protein adsorption (Lempka et al., 2009; Newbold et al., 2010). There are differences between different materials, different animals and different implant sites. However, all studies show that the electrochemical performance of electrodes *in vitro* and *in vivo* cannot be compared. As different electrode materials were used in these studies, is important to realize that proteins and cells adhere differently to surfaces depending on their micro- and nanotopography (Anselme et al., 2010; Cyster et al., 2003). It would therefore be interesting to investigate what the influence of the surface structure of the material is on its *in vivo* electrochemical properties.

CHAPTER 4. INFLUENCE OF IMPLANTATION ON A POROUS AND A SMOOTH TITANIUM NITRIDE COATING

As mentioned in the previous chapter, it is of interest to compare the *in vivo* electrochemical properties of a porous and smooth material, which was done in study III. Although it has been shown that fibroblasts preferentially adhere to smooth TiN compared to porous TiN (Cyster et al., 2003), it is extremely difficult to predict how proteins and cells respond to surface structures (Anselme et al., 2010). These results can therefore not simply be transferred to the porous TiN coating investigated in this study.

In this study, it was hypothesized that the main difference in the electrochemical properties would not be related to the amount of protein and cell adhesion. Rather, it was expected that the effect of protein and cell adhesion on the mobility of counter ions and other charged species to diffuse into and out of the pores of the porous electrodes would determine the outcome of the study. We therefore hypothesized that the electrochemical properties, especially Q_{inj}, ΔE_p and C_{pulse} of porous TiN electrodes would deteriorate more due to implantation than the electrochemical properties of smooth TiN electrodes. Of particular interest was whether the greatest relative difference between smooth and porous electrodes would be found immediately after implantation or at a later stage. Hereby information about whether protein or cell adhesion has the greatest influence on the electrochemical properties of porous compared to smooth electrodes is gained. This gives direction for optimization of the surface structure of stimulation electrodes.

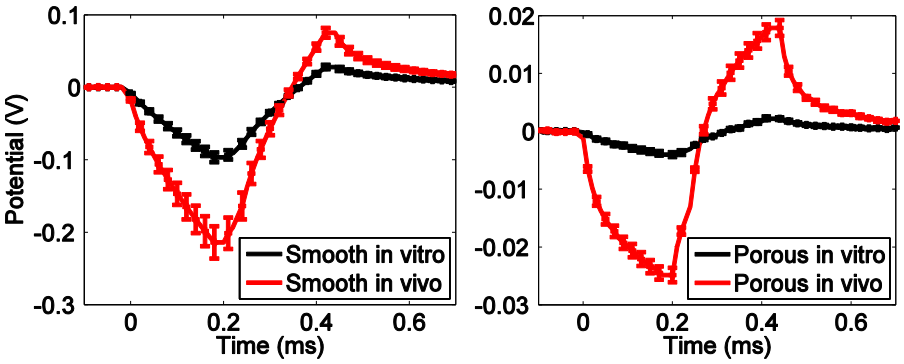

Figure 4-1 Average voltage transients of smooth (left) and porous (right) TiN electrodes measured in saline and directly after implantation. Notice the difference on the y-axis.

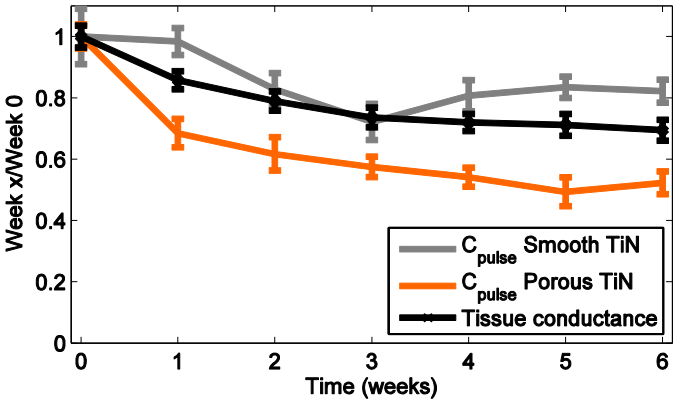

Figure 4-2 Average tissue conductance and C_{pulse} of smooth and porous TiN electrodes normalized to their values directly after implantation (week 0) as a function of time.

Figure 4-1 shows that the pulsing properties of the porous electrodes were more affected than the pulsing properties of the smooth electrodes by acute implantation compared to placement in saline. ΔE_p of the porous electrodes was 6.7±0.8 times larger *in vivo* compared to *in vitro*, while this ratio was 2.3±0.3 for the smooth TiN electrodes. The increase in ΔE_p could mostly be explained by a decrease in C_{pulse} for the smooth electrodes. The decrease in C_{pulse} is probably caused by the adhesion of biomolecules and cells to the electrode surface. This decreases the surface area available for adsorption of counter-ions (Hudak, 2011).

For the porous electrodes, the decrease in C_{pulse} is larger than for the smooth electrodes. Furthermore, the cyclic voltammogram of the porous TiN electrodes was diagonal *in vivo* at sweep rates higher than 0.5 V/s, which it was not *in vitro* (see Meijs et al., *under review*; study III). These changes are due to an increase in the pore resistance, which causes a decrease in the inner-pore surface area available for pulsing (Cogan, 2008; Norlin et al., 2005). C_{pulse} of the porous electrodes was 4.8 times smaller *in vivo* than in saline, while ΔE_p was 6.7 times larger *in vivo* than *in vitro*. The difference between these ratios is caused by the steep potential drop during the first 40 µs of the pulse (see Figure 4-1). This potential drop is likely due to the bulk electrolyte no longer being purely resistive, but having capacitive properties as well (Lempka et al., 2009; Newbold et al., 2010; Williams et al., 2007).

In order to compare the changes with time after implantation, the tissue conductance[2] and C_{pulse} were divided by their mean value directly after implantation (week 0). The tissue conductance had approximately the same values and followed the same trend for both electrode groups. The average tissue conductance of the two

[2] The tissue conductance is the inverse of the high frequency impedance (63 kHz).

groups is shown in Figure 4-2. C_{pulse} shows a decreasing trend with time for both smooth and porous TiN electrodes. C_{pulse} of the porous electrodes decreased to 52% of its C_{pulse} in week 0. C_{pulse} of the smooth electrodes was less affected and decreased to 82% of its C_{pulse} in week 0.

The changes in C_{pulse} and ΔE_p are in line with observations made using other materials and other animal models, as described in the previous chapter. There are currently no studies that have investigated a smooth and a porous electrode coating of the same material. A recent study, however, has looked at three different types of conducting polymer electrodes (Mandal et al., 2015). Although the study shows that each of these conducting polymers is differently affected by acute as well as chronic implantation, it is difficult to relate these changes to our study. Firstly, the voltage transients change dramatically during a 40 day period in saline (Mandal et al., 2015). These changes cannot be viewed separately from the changes observed *in vivo*[3]. Secondly, the electrolyte permeating the conducting polymer structure provides its mechanical stability (Mandal et al., 2015). If the electrolyte cannot permeate the conducting polymer structure, it may collapse, which has a pronounced effect on the electrochemical properties of the electrodes (Mandal et al., 2015). The influence of implantation on the electrochemical properties of the electrodes can therefore not be viewed separately from its mechanical stability.

In conclusion, the greatest difference between the smooth and porous electrodes was observed upon acute implantation, as illustrated by Figure 4-3. This means that protein adsorption had the greatest effect on pore resistance and provided the greatest limitation for charge injection using porous electrodes. Porous TiN remained capable of higher charge injection than smooth TiN. The electrodes can be improved by making wider pores, allowing proteins to diffuse in and out of the pores and decreasing the pore resistance. Another option would be to develop electrodes that are biofouling resistant.

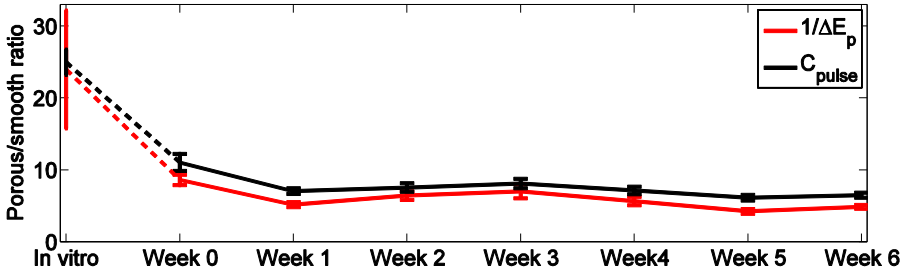

Figure 4-3 Porous/smooth ratios of the pulsing properties.

[3] During study I and II, the porous TiN coatings have been investigated in saline for the duration of the implanted period and no changes were observed in the voltage transients.

CHAPTER 5. BIOFOULING AND ELECTRICAL STIMULATION

In study IV, the influence of implantation on an electrode coating that is biofouling resistant was investigated. As shown in study I-III as well as in the literature, protein and cell adhesion cause changes in the electrochemical properties of implanted electrodes. The interference between the electrode environment and its function is called biofouling (Wisniewski et al., 2000). A material that has been reported to be biofouling resistant is boron-doped diamond (BDD) (Hudak, 2011; Trouillon & O'Hare, 2010). These studies show that the cyclic voltammogram of BDD and specifically the capacitance derived from it are not significantly different in inorganic saline compared to more complex organic solutions.

It was expected that the electrochemical properties of BDD electrodes would be less affected by acute implantation, due to resistance to biofouling in simple and complex protein solutions (Hudak, 2011; Trouillon & O'Hare, 2010). BDD electrodes become encapsulated like all implants and biomaterials (Garrett et al., 2015). However, the capsule was shown to be relatively thin (Garrett et al., 2015). It was therefore expected that the electrochemical properties of BDD electrodes would be less affected by tissue encapsulation during the chronic implantation stage. The BDD electrodes were compared to (smooth) TiN electrodes, which have electrochemical properties similar to BDD (Meijs et al., 2013) and which are susceptible to biofouling.

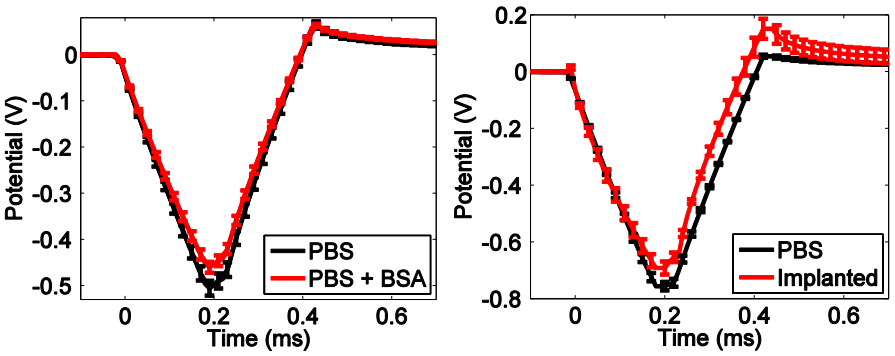

Figure 5-1 Average voltage transients of BDD electrodes in PBS without and with BSA (left) and before and after implantation (right). The difference on the axis is due to using electrode pins for the measurements in PBS and PBS+BSA (left) and using completely assembled electrodes for the measurements done before and after implantation.

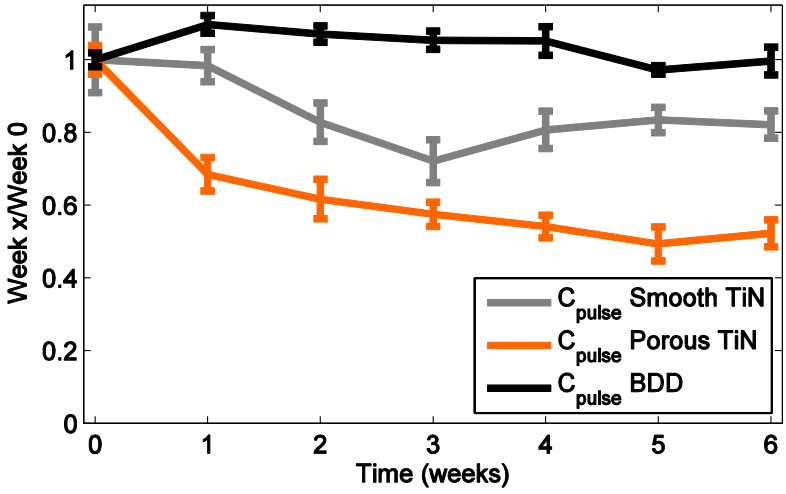

Figure 5-2 Average C_{pulse} of porous and smooth TiN and BDD electrodes normalized to their values directly after implantation (week 0) as a function of time after implantation.

The biofouling resistance of BDD and TiN electrodes was investigated in phosphate buffered saline (PBS) without and with bovine serum albumin (BSA). There was no difference in the capacitive current of BDD electrodes during CV in PBS with or without BSA (see Meijs et al., *submitted*; study IV). The capacitive current of smooth TiN electrodes, on the other hand, was smaller in PBS with BSA than without BSA. These results are comparable to previous studies (Hudak, 2011; Trouillon & O'Hare, 2010). Figure 5-1 shows that ΔE_p of the BDD electrodes was slightly smaller in PBS with BSA than in PBS without BSA. On the contrary, ΔE_p was 27% larger in PBS with BSA than without BSA for smooth TiN electrodes. These results were an indication that the pulsing properties of BDD electrodes could be less affected by implantation.

Figure 5-1 shows that the ΔE_p of the BDD electrodes was also smaller after acute implantation compared to placement in PBS. This is due to a small, but significant increase in C_{pulse}. Figure 5-2 shows that C_{pulse} of the BDD electrodes fluctuated around its acute (week 0) value, while C_{pulse} decreased as a function of time for smooth and porous TiN electrodes. BDD electrodes therefore have approximately the same Q_{inj} after implantation as in PBS. As discussed in previous chapters, this is a unique property that has not been shown for any other stimulation material.

Interestingly, BDD becomes encapsulated like any other implanted material, although a thinner capsule may be formed (Garret et al., 2015). In fact, various cell types thrive on the diamond surface (Ariano et al., 2009; Kromka et al., 2010; Nistor et al., 2015). The tissue response to BDD after implantation is therefore not fundamentally different from conventional tissue responses to biomaterials. Rather,

the electrochemical properties of BDD electrodes are unaffected by the tissue response after implantation. This is an encouraging finding, which could potentially increase the durability, safety and longevity of implanted stimulation electrodes.

One drawback of the BDD electrodes is the low C_{pulse}, which limits Q_{inj}. This can be improved by increasing the ESA of the BDD electrodes. This was done in study V by adding a 50-70 nm layer of BDD on top of a porous TiN surface. Various deposition parameters were used for the TiN coatings, resulting in ESA/GSA ratios ranging from 89 to 295. The BDD coatings were as thin as possible on all electrodes in order not to block the pores.

The CSC was approximately doubled for all TiN+BDD electrodes compared to bare TiN. The CSC increased linearly with coating thickness before and after adding the BDD layer, indicating that the BDD layer covered the entire surface area of the porous TiN and did not block the pores. Figure 5-3 shows that the increase in CSC was mostly due to the wide safe potential limits of BDD compared to TiN. C_{pulse} was lower for all electrodes with BDD compared to without (see Figure 5-4). As mentioned in section 1.2, not the entire surface area can be used under fast pulsing conditions due to a time constant (RC) for accessing the entire pore depth (Cogan, 2008; Norlin et al., 2005). This time constant depends on the electrode material, the pore width and the electrolyte (Cogan, 2008). The double layer capacitance (derived from CV) of the electrodes before and after adding the BDD layer was similar and does therefore not contribute to the time constant. The pore resistance is, however, increased by adding a thin layer of BDD on top of the TiN surface, due to the decreased pore width. This decreases the pore depth that can be accessed during stimulation and it therefore decreases C_{pulse}. The safe potential limit of BDD (-1.3 V vs Ag|AgCl) is, however, more than double the limit of TiN (-0.6 V vs Ag|AgCl). This means that Q_{inj} will also be approximately doubled using an additional layer of BDD on top of porous TiN compared to porous TiN only.

BDD with a high ESA/GSA ratio has been produced before (Bonnauron et al., 2008; Girard et al., 2012; Hebert et al., 2014; Kiran et al., 2013; Piret et al., 2015; Sun et al., 2012). The stimulation performance of these BDD electrodes, in terms of Q_{inj} and C_{pulse}, has not been evaluated. CV has been performed for BDD deposited on a carbon nanotube scaffold. This resulted in a CSC of 0.58 mC/cm^2 (Hebert et al., 2014) and 10 mC/cm^2 (Piret et al., 2015) and a double layer capacitance of 3 mF/cm^2 (Piret et al., 2015). The CSC of porous TiN+BDD ranged from 32 to 107 mC/cm^2 and the double layer capacitance ranged from 20 to 72 mF/cm^2.

Due to the large GSA of these electrodes it was not possible to determine Q_{inj}. Machine limits (± 10V) were always reached before the safe potential limits were reached. If Q_{inj} is extrapolated from the data shown in Figure 5-4, a value of ~1

µC/cm^2 would be obtained for TiN and ~1.7 µC/cm^2 for TiN+BDD[4]. This is in the range of the current state of the art in neural stimulation materials (see table 1-1). It must be remembered, however, that macro-electrodes are used for this study, making this level of performance exceptional (Cogan et al., 2007a).

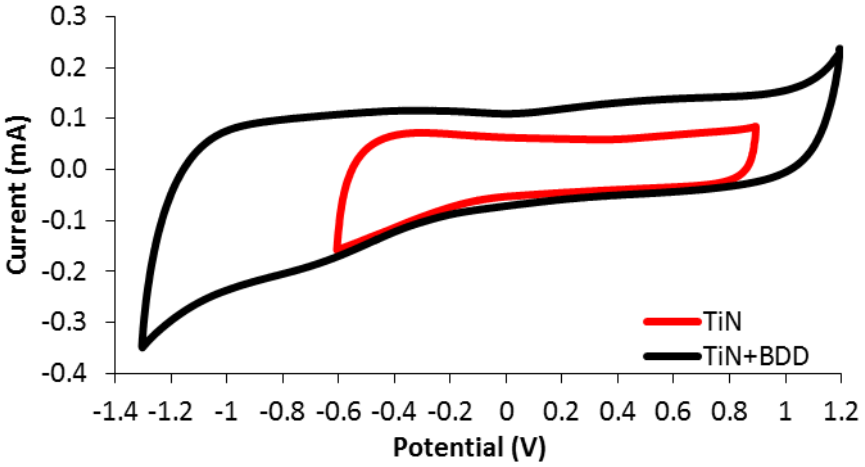

Figure 5-3 Cyclic voltammograms of a porous TiN electrode without and with BDD. TiN deposition parameters: N_2-flow=180 sccm, time=180 min, coating thickness: 2.1 µm.

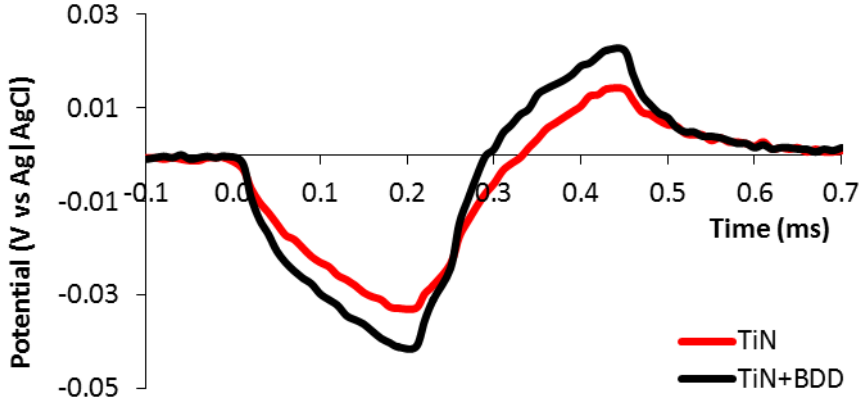

Figure 5-4 Voltage transients of a porous TiN electrode without and with BDD using a 20 mA current. TiN deposition parameters are the same as for Figure 5-3.

[4] E_{mc} was assumed to be -0.04 V for TiN and -0.05 V for TiN+BDD using a 20 mA current. The safe potential limit for each of the materials was divided by the respective $E_{mc,}$ resulting in a multiplication factor for the maximum current. This leads, however, to an extrapolation way beyond the data, so these values are very rough approximations and are only intended to compare the results to the state of the art.

CHAPTER 6. FUTURE PERSPECTIVES IN NEURAL STIMULATION ELECTRODE COATINGS

Different requirements are put on neural electrodes based on their location and purpose. For indirect neural interfaces, such as for the C-LIFE stimulation electrode, it is important the electrode maintains low stimulation thresholds and the capacity to deliver the required amount of charge after implantation. Encapsulation does not necessarily pose a problem for electrodes with an indirect neural interface, as long as charge injection limits and stimulation thresholds remain constant. It does, however, pose a problem for electrodes with a direct interface to the neurons, as encapsulation tissue creates a distance between the electrode and the target tissue.

6.1. INDIRECT NEURAL INTERFACES

Stimulation thresholds were only investigated in study I and II. These remained stable for the duration of both studies. Based on the changes in ΔE_p and C_{pulse} observed in studies I-III, it can be assumed that the amount of charge that can safely be injected decreases after implantation. In study IV, however, these changes that are typical for implanted electrodes were not observed for implanted BDD electrodes. It was therefore investigated whether the ESA of the BDD electrodes could be increased by using a porous TiN substrate. This was successful and the performance of the porous BDD electrodes is comparable to that of porous TiN electrodes *in vitro*. All Q_{inj} mentioned in table 1-1 are measured *in vitro* and it is indeed encouraging that these novel porous BDD electrodes show a comparable performance.

The aspect that is most promising about these electrodes is that they are supposedly biofouling resistant. This means that Q_{inj} would not be different *in vivo* compared to *in vitro*, which is currently not the case for any other implantable materials. One important future step is to verify this in protein solutions as well as using an animal model. Based on study III, it could be expected that Q_{inj} will be slightly smaller *in vivo* compared to *in vitro*. Since the electrodes are porous, the diffusion of charged species into and out of the pores will likely be hindered by the adhesion of proteins and cells, as it was for the porous TiN electrodes. This decreases the pore depth that can be accessed during stimulation, decreasing the surface area available for charge injection during fast pulsing. Whether this hypothesis is true and to what extent it influences Q_{inj} of porous BDD must, however, be verified *in vivo*.

The results of those studies will also have implications for the stimulation electrode that was investigated in this PhD project (see section 1.1). If Q_{inj} of porous BDD is only mildly affected by implantation compared to placement in inorganic saline, the GSA of the electrode contact can be minimized. As it is important that the electrode remains robust against movement, it is suggested that the diameter of the electrode contact is decreased.

6.2. DIRECT NEURAL INTERFACES

Electrodes implanted in direct contact with populations of neurons, for example inside the nerve or the brain, are termed direct neural interfaces. In order for such electrodes to remain functional, it is required that the neurons that are targeted stay close to the electrode surface (up to 100 μm for recording electrodes) (Polikov et al., 2005). As the electrode is implanted, however, many neurons die in the area surrounding the electrode (Green & Abidian, 2015). For the direct neural interfaces, it is not sufficient that Q_{inj} is stable after implantation. It is also not satisfactory to have a thin sheath of encapsulation tissue around the electrode, which is the case for diamond electrodes (Garret, 2015). In order to maintain a direct neural interface, recent research has focused on attracting neurons to the electrode and regenerating those neurons that did not die due to the mechanical tissue damage caused by the electrode implantation (Fattahi et al., 2014; Green & Abidian, 2015).

The conventional metals appear unsuitable for the direct neural interface, as they are intrinsically different from the biological material (Fattahi et al., 2014; Jeong et al., 2015). Organic materials are therefore of great interest, as these match the biological environment to a greater extent (Jeong et al., 2015). They can furthermore be tailored with biomolecules in order to attract and regenerate neurons (Aregueta-Robles et al., 2014; Fattahi et al., 2014; Green & Abidian, 2015). Materials that have been adapted in this way for neural stimulation and sensing purposes include carbon nanotubes, conductive polymers and hydrogels (Aregueta-Robles et al., 2014; Fattahi et al., 2014; Green & Abidian, 2015). There are, however, significant challenges to be met before these electrodes can be applied to humans. Carbon nanotubes are, for example, cytotoxic in high concentrations (Aregueta-Robles et al., 2014). Conducting polymers have shown problems with delamination and cracking (Green et al., 2012a; Venkatraman et al., 2011). They are susceptible to biofouling (Mandal et al., 2015), even more so than platinum (Green et al., 2013). And they become encapsulated by scar tissue (Cui et al., 2003). Synthetic hydrogels are promising for stimulation electrodes, as they decrease cell interaction (Aregueta-Robles et al., 2014). This could render the substrate to which they are applied biofouling resistant. Hydrogels can be made conductive for the purpose of electrical stimulation and sensing. This has been done most frequently using conductive polymers (Green et al., 2012b; Green & Abidian, 2015). Hydrogels are more mechanically compatible with soft tissues than metals. Additionally, biomolecules and cells can be incorporated in the hydrogel, which

may lead to a favorable tissue response (Fattahi et al., 2014; Green et al., 2013b). However, the mechanical stability of the hydrogel remains a problem *in vivo* that needs still to be overcome (Fattahi et al., 2014).

Diamond is also an organic material, which has been shown to be more biocompatible than silicone (Garrett et al., 2015). An exceptionally thin (median: 16 µm) capsule was formed around nitrogen included ultra-nanocrystalline diamond macro electrode implants (ø: 1 cm) (Garrett et al., 2015). A thicker capsule (median: 86 µm) was found for BDD electrodes, but it must be taken into account that these were implanted in close proximity to the positive controls (stannous octoate) (Garrett et al., 2015). This may have influenced the capsule thickness of the BDD electrodes. Although these results are encouraging, they cannot be directly translated to the direct neural interface, as this interface consists of different tissues. Diamond micro-electrode arrays have recently been implanted in the sub-retinal space of rats (Bendali et al., 2015). This study showed an increased number of bipolar cells relative to all other cells compared to polyimide and platinum (Bendali et al., 2015). Furthermore, it is possible to functionalize the diamond surface by attaching molecules to it (Härtl et al., 2004; Szuneritz & Boukherroub, 2008). This could be used to specifically attract and regenerate neurons, which has been investigated to some extent in cell cultures. The results of these efforts vary. Several authors report that functionalization of the diamond surface is not necessary and does not increase neuronal adhesion (Bendali et al., 2014; Cai et al., 2015; Edgington et al., 2013), while others report the opposite (Ojovan et al., 2014; Regan et al., 2011; Vaitkuviene et al., 2015). What matters most, however, is the relative amount of neurons adhering to the electrode surface during competitive cell adhesion *in vivo*. This has yet to be investigated for functionalized diamond.

Despite the intrinsic difference between metal and biological properties (Fattahi et al., 2014; Jeong et al., 2015), it must be mentioned that there are methods to fabricate flexible neural interface using metal contacts (Kim et al., 2014; Minev et al., 2015; Wu et al., 2015). Recently, a platinum-silicone composite and stretchable gold have been used to create a flexible and stretchable electrode, which has proven its superior functionality compared to a stiff electrode *in vivo* (Minev et al., 2015). The problem with metal electrodes remains, however, that they are biofouling susceptible and become encapsulated.

CHAPTER 7. CONCLUSIONS

At the start of this project, it was known that the pulsing properties of stimulation electrodes were different upon acute implantation for a number of electrode materials. Little was known, however, about the long term charge injection properties of implanted electrodes. The aim of this PhD project was to investigate how stimulation electrodes are affected by tissue responses.

Pulsing properties of porous TiN were, like many other electrode materials, affected by implantation. The trends observed during the implanted period resembled changes in the tissue impedance. At the time these investigations were carried out, several other studies reported changes in the pulsing properties of stimulation electrodes during chronic implantation, but none of them related these changes to the foreign body response. Various animal models with different implantation sites and different electrode materials were used. Nevertheless, the stimulation properties of all of them were affected by implantation. This appears thus to be a general problem of all stimulation electrodes regardless of where they are implanted and in which species. This might mean that clinical stimulation performed in humans exceeds safety limits determined *in vitro*, which has been suggested before by Wei & Grill (2009).

Although the electrochemical properties of the electrodes changed upon implantation, the electrodes were not damaged after implantation. In fact, the changes observed *in vivo* were largely reversed when the electrodes were explanted. This challenges whether the method of determining the safe charge injection limit can be applied *in vivo*. Other methods to determine this limit exist (Bonner et al., 1993; Musa et al., 2011) but these have not been applied *in vivo*.

Porous TiN electrodes were quite severely affected by implantation. It was therefore of interest to compare them to smooth TiN electrodes. Pulsing properties of porous TiN electrodes were more affected by tissue responses than pulsing properties of smooth TiN electrodes, especially upon acute implantation. This indicates that protein adsorption has the greatest effect on the diffusion limitation within the pores. This study is the first to compare how the electrochemical properties of a porous and a smooth material are affected by implantation. Its findings are very relevant in the design of any porous material, as all of them will likely be subject to a similar diffusion limitation to some extent. This is important to take into account when designing a porous electrode coating for a stimulation electrode. The porous coating outperforms the smooth coating throughout the implanted period. Its stimulation performance could, however, be improved by making the pores as wide as possible. Another type of surface structure, which

increases the ESA are nanotubes. As this is a more open type of structure, it might be less affected by a diffusion limitation.

In contrast to smooth and porous TiN, the pulsing properties of BDD were not affected by protein adhesion. Moreover, the pulsing properties of BDD electrodes were unaffected by tissue responses at any stage after implantation. This has not been reported before for any electrode material. This is a very interesting and promising finding for all stimulation electrodes, as the stimulation performance of all investigated electrodes have been shown to be affected by implantation. It must, however, still be investigated whether BDD remains fouling resistant regardless of implantation location.

A constraint of BDD for the use of this material in neural stimulation electrodes is that it can inject little charge compared to conventional materials (Pt, PtIr, IrOx, TiN, etc.). A 50-70 nm layer of BDD was therefore deposited on top of porous TiN, increasing its surface area more than 100 fold. This increased the capacitance of BDD to a level that is comparable to porous TiN. Moreover, due to the wide water window of BDD, Q_{inj} is likely higher for porous BDD than for porous TiN alone. This makes the performance of porous BDD comparable to the state-of-art. Taking into account that all other materials are fouling susceptible, porous BDD may exhibit the best *in vivo* stimulation performance of all of these. The next step is therefore to evaluate the biofouling resistance of the novel porous BDD electrode coatings in protein containing solutions and *in vivo*.

All in all, it is very promising that a material has been established that is biofouling resistant in terms of charge injection. This is likely to increase the safety, durability and longevity of neural implants. It might even open the way for new therapeutic stimulation methods.

LITERATURE LIST

Anderson, J. M. & McNally, A. K. (2011) Biocompatibility of implants: lymphocyte/macrophage interactions. Seminars in immunopathology, 33, 221-233.

Anderson, J. M., Rodriguez, A & Chang, D. T. (2008) Foreign body reaction to biomaterials. Seminars in immunopathology, 20, 86-100.

Anselme, K. et al. (2010) The interaction of cells and bacteria with surfaces structured at the nanometer scale. Acta Biomaterialia, 6, 3824-3846.

Aregueta-Robles, U. A. et al. (2014) Organic electrode coatings for next-generation neural interfaces. Frontiers in neuroengineering, 7, art. 16.

Ariano, P. et al. (2009) On diamond surface properties and interactions with neurons. The European physical journal E, 30, 149-156.

Aryan, N. P. et al. (2011) *In vitro* study of titanium nitride electrodes for neural stimulation. Proceedings of the 33rd IEEE EMBS annual international conference, August 30 - September 3, Boston, USA.

Aryan, N. P., Kaim, H. & Rothermel, A. (2015) Stimulation and recording electrodes for neural prostheses (Ch. 6). Springer international publishing.

Bendali, A. et al. (2014) Distinctive glial and neuronal interfacing on nanocrystalline diamond. Plos one, 9, 1-8.

Bendali, A. et al. (2015) Synthetic 3D diamond-based electrodes for flexible retinal neuroprostheses: Model, production and *in vivo* biocompatibility. Biomaterials, 67, 73-83.

Bonnauron, M. et al. (2008) High aspect ratio diamond microelectrode array for neuronal activity measurements. Diamond & related materials, 17, 1399-1404.

Bonner, M. D. et al. (1993) The pulse-clamp method for analyzing the electrochemistry on neural stimulation electrodes. Journal of the electrochemical society, 140, 2740-2744.

Brown, B. et al. (2011) Electrochemical charge storage properties of vertically aligned carbon nanotube films: the activation-enhanced length effect. Journal of the electrochemical society, 158, K217-K224.

Brunton, E. K. et al. (2015) *In vivo* comparison of the charge densities required to evoke motor responses using novel annular penetrating microelectrodes. Frontiers in Neuroengineering, 8, art. 5.

Cai, Y. et al. (2015) Strategy towards independent electrical stimulation from cochlear implants: Guided auditory neuron growth on topographically modified nanocrystalline diamond. Acta Biomateriali (In press).

Carretero, N. M. et al. (2014) IrOx carbon nanotube hybrids: a nanostructured material for electrodes with increased charge capacity in neural systems. Acta Biomaterialia, 10, 4548-4558.

Carretero, N. M. et al. (2015) Enhanced charge capacity in iridium oxide - graphene oxide hybrids. Electrochimica Acta, 157, 369-377.

Cheong, G. L. M. et al. (2014) Conductive hydrogels with tailored bioactivity for implantable electrode coatings. Acta Biomaterialia, 10, 1216-1226.

Cogan, S. F. et al. (2004) Over-pulsing degrades activated iridium oxide films used for intracortical neural stimulation. Journal of neuroscience methods, 137, 141-150.

Cogan, S. F. et al (2006) Potential-biased, asymmetric waveforms for charge-injection with activated iridium oxide (AIROF) neural stimulation electrodes. IEEE transactions on biomedical engineering, 53, 327-332.

Cogan S. F. (2006) *In vitro* and *In vivo* differences in the charge-injection and electrochemical properties of iridium oxide electrodes. Proceedings of the 28th IEEE EMBS annual international conference, August 30 – September 3, New York, USA.

Cogan, S. F. et al. (2007a) The influence of electrolyte composition on the *in vitro* charge-injection limits of activated iridium oxide (AIROF) stimulation electrodes. Journal of neural engineering, 4, 79-86.

Cogan, S. F. et al. (2007b) Corrosion resistance of stainless steel nerve cuff electrodes in the neurostep FES system. Proceedings of the 12th annual conference of the international FES society, November, Philadelphia, USA.

Cogan, S. F. (2008) Neural stimulation and recording electrodes. Annual review of biomedical engineering, 10, 275-309.

Cogan, S. F. et al. (2009) Sputtered iridium oxide films for neural stimulation electrodes. Journal of biomedical materials research part B: applied biomaterials, 89, 353-361

Cyster, L. A. et al. (2003) The effect of surface chemistry and nanotopography of titanium nitride (TiN) films on 3T3-L1 fibroblasts. Journal of biomedical materials research part A, 67, 138-147.

Edgington, R. J. et al. (2013) Patterned neuronal networks using nanodiamonds and the effect of varying nanodiamond properties on neuronal adhesion and outgrowth. Journal of neural engineering, 10, 1-9.

Farag, F. F. et al. (2012) Dorsal genital nerve stimulation in patients with detrusor overactivity: a systematic review. Current urology reports, 13, 385-388.

Fattahi, P. et al. (2014) A review of organic and inorganic biomaterials for neural interfaces. Advanced materials, 26, 1846-1885.

Fjorback, M. et al. (2009). IPC No. A61N 1/36. Patent No. WO2009080785.

Fjorback, M. V. et al. (2006) Event driven electrical stimulation of the dorsal penile/clitoral nerve for management of neurogenic detrusor overactivity in multiple sclerosis. Neurology and urodynamics, 25, 349-355.

Gabriel S., Lau, R. W. & Gabriel, C. (1996) The dielectricl properties of biological tissue: II. measurements in the frequency range 10 Hz to 20 GHz. Physics in medicine and biology, 41, 2251-2269.

Garret, D. J. et al. (2012) Ultra-nanocrystalline diamond electrodes: optimization towards neural stimulation applications. Journal of neural engineering, 9, 1-10.

Garrett, D. J. et al. (2015) *In vivo* biocompatibility of boron doped and nitrogen including conductive-diamond for use in medical implants. Journal of biomedical materials research part B: applied biomaterials, 00, 000-000.

Girard, H. A. et al. (2012) Electrostatic grafting of diamond nanoparticles towards 3D diamond structures. Diamond & related materials, 23, 83-87.

Goldman, H. B. et al. (2008) Dorsal genital nerve stimulation for the treatment of overactive bladder symptoms. Neurology and urodynamics, 27, 499-503.

Green R. & Abidian, M. R. (2015) Conducting polymers for neural prosthetic and neural interface applications. Advanced materials, 27, 7620-7637.

Green, R. A. et al. (2012) Conductive hydrogels: mechanically robust hybrids for use as biomaterials. Macromolecular bioscience, 12, 494-501.

Green, R. A. et al. (2013a) Performance of conduction polymer electrodes for stimulating neuroprosthetics. 10, 1-11.

Green, R. A. et al. (2013b) Living electrodes: tissue engineering the neural interface. Proceedings of the 35th IEEE EMBS annual international conference, July 3 – 7, Osaka, Japan.

Grill, W. M. & Mortimer, J. T. (1994) Electrical properties of implant encapsulation tissue. Annals of biomedical engineering, 22, 23-33.

Guex, A. A. et al. (2015) Conducting polymer electrodes for auditory brainstem implants. Journal of materials chemistry B, 3, 5021-5027.

Härtl, A. et al. (2004) Protein-modified nanocrystalline diamond thin films for biosensor applications. Nature materials, 3, 736-742.

Hassarati R. T. et al. (2014) Improving cochlear implant propreties through conductive hydrogel coatings. IEEE transactions on neural systems and rehabilitations engineering, 22, 411-418.

Hébert, C et al. (2014) Boosting the electrochemical properties of diamond electrodes using carbon nanotube scaffolds. Carbon, 71, 27-33.

Heim, M., Yvert, B. & Kuhn, A. (2012) Nanostructuration strategies to enhance microelectrode array (MEA) performance for neuronal recording and stimulation. Journal of physiology-Paris, 106, 137-145.

Hudak, E. M. (2011) Electrochemical evaulation of platinum and diamond electrodes for neural stimulation. (Electronic Thesis or Dissertation) Retrieved from https://etd.ohiolink.edu/.

Jackson A. & Zimmerman J. B. (2012) Neural interfaces for the brain and spinal cord – restoring motor function. Nature reviews neurology, 8, 690-699.

Jeong, J. W. et al. (2015) Soft materials in neuroengineering for hard problems in neuroscience. Neuron, 86, 175-186.

Kane S. R. et al. (2011) Electrical performance of penetrating microelectrodes chronically implanted in cat cortex. Proceedings of the 33rd IEEE EMBS annual international conference, August 30 - September 3, Boston, USA.

Kane, S. R. et al. (2013) Electrical performance of penetrating microelectrodes chronically implanted in cat cortex. IEEE transactions on biomedical engineering, 60, 2153-2160.

Kim, R. & Nam, Y. (2015) Electrochemical layer-by-layer approach to fabricate mechanically stable platinum black microelectrode using a mussel-inspired poly-dopamine adhesive. Journal of neural engineering, 12, 1-10.

Kim, S. (2014) Boron-doped diamond electrodes for neural stimulation. (Electronic Thesis or Dissertation) Retrieved from https://etd.ohiolink.edu/.

Kim, J. et al. (2014) Next-generation flexible neural and cardiac electrode arrays. Biomedical engineering letters, 4, 95-108.

Kiran, R. et al. (2013) Nanograss boron-doped diamond microelectrode arrays for recording and stimulating neural tissues. Transducers, June 16-20, Barcelona, Spain.

Kromka, A. et al. (2010) Semiconducting to metallic-like boron doping of nanocrystalline diamond films and its effect on osteoblastic cells. Diamond & related materials, 19, 190-195.

Lempka, S. F. (2009) *In vivo* impedance spectroscopy of deep brain stimulation electrodes. Journal of neural engineering, 6, 1-11.

Leung, R. T. et al. (2015) *In vivo* and *in vitro* comparison of the charge injection capacity of platinum macroelectrodes. IEEE transactions on biomedical engineering, 62, 849-857.

Lu, Y. et al. (2010) Electrodeposited polypyrrole/carbon nanotubes composite films electrodes for neural interfaces. Biomaterials, 31, 5169-5181.

Luo, X. et al. (2011) Highly stable carbon nanotube doped poly(3,4-ethylenedioxythiophene) for chronic neural stimulation. Biomaterials, 32, 5551-5557.

Mandal, H. S. et al. (2015) Improved poly(3,4-ethylenedioxythiophene) (PEDOT) for neural stimulation. Neuromodulation, 18, 657-663.

Martens, F. M. J. (2011) Diagnosis of neurogenic detrusor overactivity and treatment with conditional electrical stimulation of the dorsal genital nerves. (Electronic thesis or dissertation) Retrieved from http://repository.ubn.ru.nl/

Martens, F. M. J., Heesakkers, J. P. F. A & Rijkhoff, N. J. M (2011) Minimal invasive electrode implantation for stimulation of the dorsal genital nerve in neurogenic detrusor overactivity. Spinal cord, 49, 566-572.

Meijs, S. et al. (2013) Electrochemical characterization of boron-doped nanocrystalline diamond electrodes for neural stimulation. 6th international IEEE EMBS Conference on Neural Engineering, November 6-8, San Diego, USA.

Minev, I. R. et al. (2015) Electronic dura mater for long-term multimodal neural interfaces. Science, 347, 159-163.

Minnikanti, S. et al. (2010) *In vivo* electrochemical characterization and inflammatory response of multiwalled carbon nanotube-based electrode in rat hippocampus. Journal of neural engineering, 7, 1-11.

Miocinovic, (2013) History, mechanisms and applications of deep brain stimulation. JAMA neurology, 70, 163-171.

Musa, S. et al (2009) *In vitro* and *in vivo* electrochemical characterization of a microfabricated neural probe. Proceedings of the 31st IEEE EMBS annual international conference, September 2-6, Minneapolis, USA.

Musa, S. et al. (2010) Using reciprocal derivative chronopotentiometry as a technique to determine safe charge injection limits of electrodes used for neural stimulation. Proceedings of the 32nd IEEE EMBS annual international conference, August 31 – September 4, Buenos Aires, Argentina.

Musa, S. et al. (2011) Coulometric detection of irreversible electrochemical reactions occurring at Pt microelectrodes used for neural stimulation. Analytical chemistry, 83, 4012-4022.

Navarro, X. et al (2005) A critical review of interfaces with the peripheral nervous system for the control of neuroprostheses and hybrid bionic systems. Journal of the peripheral nervous system, 10, 229-258.

Negi, S. et al. (2010a) *In vitro* comparison of sputtered iridium oxide and platinum-coated neural implantable microelectrode arrays. Biomedical materials, 5, 1-9.

Negi, S. et al. (2010b) Neural electrode degradation from continuous electrical stimulation: comparison of sputtered and activated iridium oxide. Journal of neuroscience methods, 186, 1-8.

Newbold, C. et al. (2010) Changes in biphasic electrode impedance with protein adsorption and cell growth. Journal of neural engineering, 7, 1-11.

Nistor, P.A. et al. (2015) Long-term culture of pluripotent stem-cell-derived human neurons on diamond – A substrate for neurodegeneration research and therapy. Biomaterials, 61, 139-149.

Norlin, A., Pan, J. & Leygraf, C. (2005) Investigation of electrochemical behavior of stimulation/sensing materials for pacemaker electrode applications: I. Pt, Ti, and TiN coated electrodes. Journal of the electrochemical society, 152, J7-J15.

Ojovan, S. M. et al. (2014) Nanocrystalline diamond surface for adhesion and growth of primairy neurons, conflicting results and rational explanation. Frontiers in neuroengineering, 7, art. 17.

Pan, Y. L. et al. (2013) Sputtering condition optimization sputtered IrOx and TiN stimulus electrodes for retinal prosthesis. IEEJ transactions on electrical and electronic engineering, 8, 310-312.

Park, S. et al. (2010) Nanoporous Pt microelectrode for neural stimulation and recording: in vitro characterization. Journal of physical chemistry, 114, 8721-8726.

Piret, G. et al. (2015) 3D nanostructured boron-doped diamond for microelectrode array neural interfacing. Biomaterials, 53, 173-183.

Polikov, S. V., Tresco, P. A. & Reichert, W. M. (2005) Response of brain tissue to chronically implanted neural electrodes. Journal of neuroscience methods, 148, 1-18.

Regan, E.M. et al. (2011) Spatially controlling neuronal adhesion and inflammatory reactions on implantable diamond. IEEE journal on emerging and selected topics in circuits and systems, 1, 557-565.

Samba, R., Herrmann, T. & Zeck, G. (2015) PEDOT-CNT coated electrodes stimulate retinal neurons at low voltage amplitudes and low charge densities. Journal of neural engineering, 12, 1-11.

Stieglitz, T. & Meyer, J. U. (2006) Neural implants in clinical practice. In G. A. Urban (Ed.), BIOMEMS (Ch. 3). Dordrecht: Springer-Verlag.

Sun, J. et al. (2012) Boron doped diamond electrodes based on porous Ti substrates. Materials letters, 83, 112-114.

Szuneritz, S. & Boukherroub, R. (2008) Different strategies for functionalization of diamond surfaces. Journal of solid state electrochemistry, 12, 1205-1218.

Terasawa, Y. et al. (2013) Safety assessment of semichronic suprachoroidal electrical stimulation to rabit retina. Proceedings of the 35th IEEE EMBS annual international conference, July 3 – 7, Osaka, Japan.

Tian, H. C. et al. (2014a) Graphene oxide doped conducting polymer nanocomposite film for electrode-tissue interface. Biomaterials, 35, 2120-2129.

Tian, H. C. et al. (2014b) Biotic and abiotic molecule dopants determining the electrochemical performance, stability and fibroblast behavior of conducting polymer for tissue interface. The royal society of chemistry advances, 4, 4761-4771.

Trouillon, R. & O'Hare, D. (2010) Comparison of glassy carbon and boron doped diamond electrodes: Resistance to biofouling. Electrochimica Acta, 55, 6586-6595.

Tyler, D. J. & Polasek, K. H. (2009) Electrodes for the neural interface. In E. S. Krames, P. H. Peckham & A. R. Rezai (Eds.) Neural Engineering. London: Academic Press.

Vaitkuviene, A. et al. (2015) Impact of differently modified nanocrystalline diamond on the growth of neuroblastoma cells. New biotechnology, 32, 7-12.

Van Breda, J. et al. (2014) Pilot study of subject controlled percutaneous dorsal genital nerve stimulation for the treatment of idiopathic urgency incontinence. 44th Annual meeting of the international continence society, October 20-24, Rio de Janeiro, Brazil.

Venkatraman, S. et al. (2011) *In vitro* and *in vivo* evaluation of PEDOT microelectrodes for neural stimulation and recording. IEEE transactions on neural systems and rehabilitation engineering, 19, 307-316.

Wei, X. F. & Grill, W. M. (2009) Impedance characteristics of deep brain stimulation electrodes *in vitro* and *in vivo*. Journal of neural engineering, 2009, 1-9.

Weiland, J. D., Anderson, D. J. & Humayun, M. S. (2002) *In vitro* electrochemical properties for iridium oxide versus titanium nitride stimulating electrodes. IEEE transactions on biomedical engineering, 49, 1574-1579.

Weremfo, A. et al. (2015) Investigating the interfacial properties of electrochemically roughened platinum electrodes for neural stimulation. Langmuir, 31, 2593-2599.

Williams, J. C. et al. (2007) Complex impedance spectroscopy for monitoring tissue responses to inserted neural implants. Journal of neural engineering, 4, 410-423.

Wisniewski, N., Moussy, F. & Reichert, W. M. (2000) Characterization of implantable biosensor membrane fouling. Fresenius' journal of analytical chemistry, 366, 611-621.

Wu, F. et al. (2015) Silk-backed structural optimization of high-density flexible intracortical neural probes. Journal of microelectromechanical systems, 24, 62-69.

Zhou, D.& Greenbaum, E. (2009) Implantable neuroprostheses 1 - Devices and applications. New York: Springer science+business media.

Zhou D. & Greenberg R. J. (2011) Electrochemistry in neural stimulation by biomedical implants. Electrochemistry, 17, 249-262.

Zhou, D. & Greenberg, R. J. (2003) Electrochemical characterization of titanium nitride microelectrode arrays for charge-injection applications. Proceedings of the 25th IEEE EMBS annual international conference, September 17-21, Cancun, Mexico.

Zhou, H. et al. (2013a) Poly(3,4-ethylenedioxythiophene)/multiwall carbon nanotube composite coatings for improving the stability of microelectrodes in neural prostheses applications. Acta biomaterialia, 9, 6439-6449

APPENDICES

I. Meijs, S., Fjorback, M., Jensen, C., Sørensen, S., Rechendorff, K., & Rijkhoff, N.J.M. (2015) Electrochemical properties of titanium nitride nerve stimulation electrodes: an *in vitro* and *in vivo* study. *Frontiers in Neuroscience, 9*, [268]. 10.3389/fnins.2015.00268

II. Meijs, S., Fjorback, M., Jensen, C., Sørensen, S., Rechendorff, K., & Rijkhoff, N.J.M. (*under review*) Influence of fibrous encapsulation on electro-chemical properties of TiN electrodes. *Submitted to Medical Engineering and Physics*.

III. Meijs, S., Sørensen C., Sørensen, S., Rechendorff, K., Fjorback, M., & Rijkhoff, N.J.M. (*submitted*) Influence of implantation on the electrochemical properties of smooth and porous TiN coatings for stimulation electrodes. *Submitted to Journal of Neural Engineering*

IV. Meijs, S., Alcaide, M., Sørensen C., McDonald, M., Sørensen, S., Rechendorff, K., Gerhardt, A., Nesladek, M., Rijkhoff, N.J.M. & Pennisi, C.P. (*submitted*) Biofouling resistance of boron-doped diamond neural stimulation electrodes is superior to titanium nitride electrodes *in vivo*. *Submitted to Journal of Neural Engineering*

V. Meijs, S., McDonald, M., Sørensen, S., Rechendorff, K., Petrák, V., Nesládek, M., Rijkhoff, N.J.M., Pennisi, C.P. (2015) Increased charge storage capacity of titanium nitride electrodes by deposition of boron-doped nanocrystalline diamond films. In *Proceedings of the 3rd neurotechnix conference*, 16-17 November 2015, Lisbon.

ISSN (online): 2246-1302
ISBN (online): 978-87-7112-448-4

AALBORG UNIVERSITY PRESS